Can. J. Remote Sensing, Vol. 35, No. 2, pp. 166–188, 2009

Linking foliage spectral responses to canopy-level ecosystem photosynthetic light-use efficiency at a Douglas-fir forest in Canada

Elizabeth M. Middleton, Yen-Ben Cheng, Thomas Hilker, T. Andrew Black, Praveena Krishnan, Nicholas C. Coops, and Karl Fred Huemmrich

Abstract. The light-use efficiency (LUE) of a mature Canadian Douglas-fir forest (DF49) was studied using high-resolution in situ temporal, spatial, and spectral measurements in conjunction with fluxes acquired from an instrumented tower. We examined the photochemical reflectance index (PRI), a spectral index responsive to high light conditions that alters reflectance at 531 nm, in combination with several alternative reference bands at 551, 570, and 488 nm. These indices were derived from directional reflectance spectra acquired by a hyperspectral radiometer system mounted on the DF49 tower, viewing the canopy through almost 360° rotations multiple times an hour daily throughout the 2006 growing season. From canopy structure information, three foliage sectors within the canopy were delineated according to instantaneous illumination conditions (sunlit, shaded, and mixed shaded–sunlit). On sunny days, the PRI indices for the sunlit foliage sector captured high light-induced stress responses, expressed as significantly different PRI values for sunlit versus shaded foliage. This difference was not observed on highly diffuse or overcast days. PRIs on sunny days tracked the diurnal photoregulation responses throughout the growing season in concert with illumination intensity. We computed the effective instantaneous LUE for the three foliage groups ($LUE_{foliage}$) using modeled and measured information. We provide convincing evidence that $LUE_{foliage}$ can be well described and strongly related to all variations of the PRI within this coniferous forest under relatively clear skies ($0.59 > r^2 > 0.80$, $P < 0.0001$). $LUE_{foliage}$ varied through the growing season between 0.015 and 0.075 μmol C μmol^{-1} absorbed photosynthetically active radiation (APAR), and the lowest daily values were associated with the sunlit foliage group. The mixed sunlit–shaded foliage was the only group to exhibit monthly averages close to the maximum ecosystem LUE parameter (ε_{max}) used in LUE models for evergreen needle forests (0.0196 μmol C μmol^{-1} APAR). Implications for remote sensing of carbon uptake dynamics and the interaction of canopy structure and physiology are discussed.

Résumé. L'efficacité d'utilisation de la lumière (LUE) d'une forêt mature canadienne de pins Douglas (DF49) a été étudiée en utilisant des mesures in situ temporelles, spatiales et spectrales à haute résolution conjointement avec des flux acquis à partir d'une tour d'instrumentation. Nous avons examiné l'indice de réflectance photochimique (PRI), un indice spectral sensible aux conditions de lumière intense qui modifie la réflectance à 531 nm, en combinaison avec plusieurs bandes de référence alternatives à 551, 570 et 488 nm. Ces indices ont été dérivés de spectres de réflectance directionnels acquis par un système radiométrique hyperspectral monté sur la tour DF49 et qui permet de visionner le couvert en effectuant des rotations de 360° plusieurs fois par heure de façon quotidienne tout au long de la saison de croissance de 2006. À partir de l'information sur la structure du couvert, trois secteurs de feuillage à l'intérieur du couvert ont été délimités en fonction des conditions instantanées d'éclairement (illuminés par le soleil, ombragés et mélange ombragé–éclairé). Les jours ensoleillés, les indices PRI pour le secteur de feuillage éclairé a enregistré des réponses élevées de stress induit par la lumière, qui s'exprimaient par des valeurs significativement différentes de PRI pour les feuillages éclairés vs les feuillages ombragés. Cette différence n'a pas été observée durant les jours caractérisés par une diffusion élevée ou les jours nuageux. Les valeurs de PRI durant les jours ensoleillés ont permis de suivre les réponses diurnes de photorégulation au cours de la saison de

Received 24 July 2008. Accepted 16 January 2009. Published on the Web at http://pubs.nrc-cnrc.gc.ca/cjrs on 5 June 2009.

E.M. Middleton[1] and Y.-B. Cheng. Biospheric Sciences Branch, National Aeronautics and Space Administration, Goddard Space Flight Center, Greenbelt, MD 20771, USA.

T. Hilker and N.C. Coops. Faculty of Forest Resources Management, University of British Columbia, Vancouver, BC V6T 1Z4, Canada.

T.A. Black. Faculty of Land and Food Systems, University of British Columbia, Vancouver, BC V6T 1Z4, Canada.

P. Krishnan. Faculty of Land and Food Systems, University of British Columbia, Vancouver, BC V6T 1Z4, Canada; and Atmospheric Turbulence and Diffusion Division, National Oceanic and Atmospheric Administration, Oak Ridge, TN 37830, USA.

K.F. Huemmrich. Joint Center for Earth Systems Technology, University of Maryland, Baltimore County, Catonsville, MD 21228, USA.

[1]Corresponding author (e-mail: Elizabeth.M.Middleton@nasa.gov).

croissance de concert avec l'intensité d'éclairement. Nous avons calculé la valeur de LUE effective instantanée pour les trois groupes de feuillage ($LUE_{foliage}$) en utilisant l'information modélisée et mesurée. Nous avons apporté une preuve convaincante à l'effet que la valeur de $LUE_{foliage}$ peut être bien décrite et fortement reliée à toutes les variations de PRI à l'intérieur de la forêt de conifères dans des conditions de ciel relativement clair ($0{,}59 > r^2 > 0{,}80$, $P < 0{,}0001$). $LUE_{foliage}$ variait tout au long de la saison de croissance entre 0,015–0,075 µmol C µmol^{-1} APAR et les valeurs quotidiennes les plus basses étaient associées au groupe de feuillage éclairé. Le feuillage mixte éclairé/ombragé a été le seul groupe à exhiber des moyennes mensuelles proches du paramètre LUE maximum de l'écosystème(ε_{max}) utilisé dans les modèles LUE pour les forêts de conifères (0,0196 µmol C µmol^{-1} APAR). Les implications pour la télédétection de la dynamique de l'absorption du carbone et des interactions de la structure et de la physiologie du couvert sont abordées.
[Traduit par la Rédaction]

Introduction

Can terrestrial ecosystem physiological function be adequately monitored remotely with spectral observations? We ask this question because direct retrieval of the functional carbon uptake status of vegetation has not been highly successful with broadband spectral indices acquired by ground or satellite-based radiometers at any spatial scale. However, continuous high spectral resolution (i.e., hyperspectral) reflectance sensors, or those having well-chosen physiologically responsive narrow bands, offer this exciting possibility (e.g., Grace et al., 2007). In particular, the photosynthetic light-use efficiency (LUE) of vegetation has been monitored successfully by the photochemical reflectance index (PRI) (Gamon et al., 1990; 1992; 1993; 1997; 2001), a spectral index based on two narrow (3–10 nm) green wavelengths. Therefore, we examine in detail the temporal and spatial dynamics of PRI with a high-resolution spectral and spatial in situ dataset, in conjunction with LUE determined from measurements at an instrumented tower, to evaluate the potential for using remote sensing to monitor physiological responses affecting carbon uptake at the ecosystem scale.

Several variations of the PRI were examined here, using in situ hyperspectral reflectance measurements made of a coniferous forest canopy, coincident with flux measurements, and which sampled the forest's instantaneous bidirectional reflectance function (BRDF). We assumed that the forest canopy structure affected the instantaneous illumination conditions within the forest canopy, potentially influencing the LUE and PRI relationships for the sunlit versus shaded foliage sectors, from which we posed the following hypotheses: (1) the PRI is capable of distinguishing physiological responses associated with excess light (e.g., high light stress) for sunlit foliage, as compared to relatively unstressed, shaded foliage; (2) the PRI of foliage can be related to tower-based estimates of gross canopy LUE; (3) a variation of the original PRI may also be useful for detecting photosynthetic down-regulation under high light; and (4) the PRI and LUE of foliage ($LUE_{foliage}$) both vary diurnally and seasonally in concert with illumination conditions.

LUE concept

Although many environmental factors are involved in photosynthetic efficiency, the most important are the intensity and duration of the incoming solar radiation regime. These are captured in the traditional LUE model (Monteith, 1972; 1977), a measure of the plant's ability to capture atmospheric carbon dioxide (CO_2) and convert it into biomass using solar energy. LUE (or ε) is defined as the ratio of gross primary production (GPP) to the amount of incident photosynthetically active radiation (PAR, 400–700 nm) absorbed over a given time period:

$$\varepsilon = \frac{\mathrm{GPP}}{\mathrm{PAR} \times f_{\mathrm{APAR}}} \tag{1}$$

where the denominator, the product of PAR and the fraction of absorbed PAR (f_{APAR}), yields the absorbed PAR (APAR) potentially available for photosynthesis. GPP, PAR, and APAR are flux densities often expressed in units of µmol·m^{-2}·s^{-1}; f_{APAR} is dimensionless, ranging between 0 and 1; and LUE can be expressed in several different units (e.g., µmol CO_2 µmol^{-1} PAR, g C MJ^{-1} PAR, or µmol C µmol^{-1} PPFD, the photosynthetic photon flux density). This LUE concept was originally demonstrated for crops over a growing season, when LUE could be determined from the biomass at harvest and the seasonally integrated APAR obtained from field instruments.

With the establishment of instrumented flux tower networks that continuously monitor carbon, water, and energy fluxes of ecosystems globally (e.g., Baldocchi et al., 2001; Baldocchi, 2003; Papale et al., 2006), the LUE concept can now be investigated for any time period of interest and applied as well to perennial vegetation that is not harvested, such as standing forests (Whitehead and Gower, 2001; Turner et al., 2003; Ahl et al., 2004; Lagergren et al., 2005; Schwalm et al., 2006; Yuan et al., 2007; Jenkins et al., 2007). However, LUE determined from eddy covariance measurements describes the response of the entire ecosystem (overstory, understory, substrate), where efficiency is expressed in terms of either net primary production (NPP) or GPP, as NPP/APAR or GPP/APAR. GPP is NPP plus the carbon lost to ecosystem respiration, estimated from indirect methods (Black et al., 1996; Goulden et al., 1997). From tower fluxes, Turner et al. (2003) found that seasonal LUE means (based on monthly growing season data) for a grassland, a hardwood forest, and a boreal black spruce forest were 1.7 ± 0.40, 1.8 ± 0.08, and 1.0 ± 0.05 g C MJ^{-1} PAR, respectively. In a mature aspen forest, the daily area-averaged

summertime LUE (as GPP efficiency) at a Fluxnet Canada site ranged between 0.004 and 0.018 μmol CO_2 μmol^{-1} PAR in 2001–2003 (Drolet et al., 2005), or reported as a growing season average over 5 years (2001–2005) at 0.0241 μmol C μmol^{-1} PPFD (Zhang et al., 2009). The latter approach provides values equivalent to those obtained from the research presented in this paper, expressed as μmol C μmol^{-1} APAR.

Instantaneous, daily, or weekly integrated LUE provide a critical indicator of vegetation health and describe the integrated ecosystem's response to contemporary environmental stress factors, as defined by plant physiologists (e.g., Zarco-Tejada et al., 2002; Lichtenthaler, 1996; Larcher, 1987), such as high light intensity, unfavorable temperatures, nutrient deficiency, and atmospheric vapor pressure deficit. These factors can be taken into account by carbon models that treat LUE as a down-regulation coefficient to optimal photosynthesis (e.g., Potter et al., 1993), but that manner of LUE determination relies on fixed look-up-table (LUT) values for assumed maximum LUE and requires a wealth of environmental information (Heinsch et al., 2003; 2006).

PRI and xanthophyll photoprotective responses

The PRI expresses the relative down-regulation of photosynthesis induced primarily by high light intensities, but it also is affected by secondary or compounding factors such as drought (Peñuelas et al., 1994; Suárez et al., 2008). The original formulation of the PRI is a normalized difference spectral index using the physiologically active 531 nm wavelength and a reference wavelength (REF λ) at 570 nm, or PRI_{570}. Several other REF λ, such as 551 nm and 488 nm, have been used to yield PRI_{551} or PRI_{488} and applied to available satellite bands (Drolet et al., 2005; 2008a). The general form for the PRI is

$$PRI_{REF\ \lambda} = [\rho 531 - \rho(REF\ \lambda)]/[\rho 531 + \rho(REF\ \lambda)] \qquad (2)$$

The physiological responses captured by the PRI are linked to the xanthophyll cycle, a biochemical interconversion of specialized carotenoid pigments bound to the photosystem II (PSII) light-harvesting complexes of chloroplasts. The primary function of the xanthophyll cycle is the prevention of oxidative damage to the photosynthetic apparatus imbedded in the chloroplasts' thylakoid membranes (Bilger et al., 1989; Pfundel and Bilger, 1994; Demmig-Adams, 1990; Adams and Demmig-Adams, 1994; Demmig-Adams and Adams, 1992; 1996; 2006; Demmig-Adams et al., 1996; Adams et al., 1999; 2002). This reversible biochemical cycle begins with a light-induced lowering of lumen pH that initiates the sequential de-epoxidization (i.e., removal of epoxide side groups, a double-bonded oxygen atom) of the xanthophyll violaxanthin (V); this occurs in two steps through conversions first to antheraxanthin (A) and then to zeaxanthin (Z). The dependence of xanthophyll de-epoxidation state on lumen pH has been described quantitatively by Pfundel and Dilley (1993). Z binds to PSII proteins, causing a conformational change that quenches excess excitation energy (Havaux and Niyogi, 1999). The fraction of PSII antennae complexes in the chloroplasts that are bound to Z, and therefore actively involved in quenching of excess radiation, has been expressed quantitatively (Gilmore and Yamasaki, 1998). In the dark, Z reverts to V through two epoxidation steps. This pigment cycle has been examined for conifers (Kurasová et al., 2003; Öquist and Huner, 2003; Štroch et al., 2008). Since A and Z have higher absorption coefficients than V at ~531 nm (Bilger and Björkman, 1990), reflectance decreases and a lower PRI_{570} value is produced when A and Z accumulate in the thylakoid membrane under high light. This nonphotochemical quenching mechanism involving the interconversion of V to Z under light and dark regimes was described by Müller et al. (2001).

With PRI_{570}, short-term responses to high light conditions (i.e., high light-induced stress) are indicated by relatively lower values (for this study, those that fall below approximately –0.02), and greater photosynthetic down-regulation is indicated by the lowest observed values (for this study, the most negative values, ≤–0.08). This is also the case for PRI_{551} (but with a shift to more negative values here), whereas the reverse situation occurs with PRI_{488}, for which increasingly greater down-regulation is indicated with larger positive values. The use of the PRI for LUE monitoring was first documented at the leaf level by Gamon et al. (1990; 1992; 1993; 1997) and substantiated by many others (Peñuelas et al., 1994; 1995; 1997; Filella et al., 1996; Trotter et al., 2002; Guo and Trotter, 2004; Evain et al., 2004; Inoue and Peñuelas, 2006; Meroni et al., 2008a; 2008b; Inoue et al., 2008). Although the PRI signal is relatively weak compared with red edge spectral indices, it has successfully been observed remotely over forests from aircraft and towers (Nichol et al., 2000; 2002; Rahman et al., 2001; Louis et al., 2005; Hilker et al., 2008c; Hall et al., 2008; Grace et al., 2007; Suárez et al., 2008) and from satellites (Drolet et al., 2005, 2008a; Rahman et al., 2004; Verrelst et al., 2008).

If the xanthophyll photoprotection mechanism is the dominant process driving instantaneous LUE, then it should vary with PAR intensity and time of day and exhibit different LUE for sunlit versus shaded leaves. However, high light intensities can be damaging to the photosystems of both sun and shade leaves if water or nutrients are not sufficiently available or if temperatures are unfavorable. Optimal PAR levels for photosynthesis in foliage of most species of higher plants typically range from 1200 to 2000 $\mu mol \cdot m^{-2} \cdot s^{-1}$ for "sun" leaves, that is, leaves that grow in the exposed light environment found in the upper and outer foliage of a plant canopy (Jones, 1983). Optimal PAR levels are lower for "shade" leaves that grow in the lower or inner portions of a canopy where shading dominates. Shaded foliage also receives a higher proportion of PAR as diffuse radiation (Alton et al., 2007). The physiological and morphological differences of sun and shade foliage have been well documented, especially concerning leaf anatomy and pigment concentrations (Boardman, 1977; Lichtenthaler et al., 1981; 2007; Thayer and Björkman, 1990; Zhang et al., 1995; Demmig-Adams, 1998;

Demmig-Adams et al., 1998; Špunda et al., 1998; Sarijeva et al., 2006; Brodersen et al., 2008). However, it should be noted that unfavorable environmental conditions such as insufficient water and nutrient levels and low–high temperatures also produce lower LUE, possibly also contributing to responses mediated through the xanthophyll cycle.

Current study focus

In our recent investigations using moderate-resolution imaging spectroradiometer (MODIS) (Justice et al., 1998) data and fluxes from towers in the Canadian Carbon Program located in Saskatchewan, we found that the viewing direction (backscattering versus forward scattering) was an important factor influencing the PRI value obtained from MODIS imagery (Drolet et al., 2005; 2008a). We also determined from modeling exercises that the canopy shadow fraction was strongly related to the PRI value retrieved, with sunlit canopy displaying lower PRI than shadowed canopy (Drolet et al., 2008a), a finding that revealed that canopy three-dimensional structure was affecting the canopy PRI–LUE relationships. This is consistent with other studies showing that the PRI retrieved from aircraft platforms is influenced by canopy structure, background reflectance, and (or) illumination and view geometry (Barton and North, 2001; Rahman et al., 2001; Nichol et al., 2002; Sims and Gamon, 2002; Guo and Trotter, 2004; Louis et al., 2005; Suárez et al., 2008).

Our eventual goal is to relate the understanding gained from in situ measurements gathered from this and related studies to improve our interpretation of satellite observations for carbon studies. The near-term goal for this study was to rigorously evaluate the spectral responses of canopy foliage sectors having different light environments in a coniferous forest stand and relate the PRI to tower LUE. To resolve the PRI dynamics of sunlit and shaded foliage and their influence on remotely sensed observations, we drew upon an existing in situ dataset comprised of high-resolution spectral, temporal, and spatial information. This dataset treasure (Hilker et al., 2008a; 2008b; 2008c) was collected in 2006 in a well-studied Douglas-fir forest (DF49) at a flux tower site in the Canadian Carbon Program flux network (Drewitt et al., 2002; Parker et al., 2004; Morgenstern et al., 2004; Humphreys et al., 2006; Jassal et al., 2007; Coops et al., 2007a; 2007b; Cai et al., 2008; Krishnan et al., 2009).

In recently published works, we provided initial evidence from select examples that the PRI_{570} for sunlit canopy is lower than that for shaded canopy sectors at this coniferous site, and we demonstrated that the PRI signal can be attributed to a physiological response rather than to one of the possible confounding factors (Hall et al., 2008; Hilker et al., 2008a). In the current study, we investigate how several variations of the PRI behave throughout a growing season using canopy spectra, fluxes, and related measurements acquired from the tower. In particular, we examined how PRI_{570}, PRI_{551}, and PRI_{488} vary diurnally and seasonally in the solar principal plane (SPP) and at the cross-plane–SPP juncture (**Figure 1**). Thus, we examined sunlit foliage dominating the BRDF "hotspot" and shaded foliage dominating the BRDF "darkspot" at opposite positions along the SPP and a mixture of intermediately located sunlit–shaded foliage. From these observations, and tower-based flux

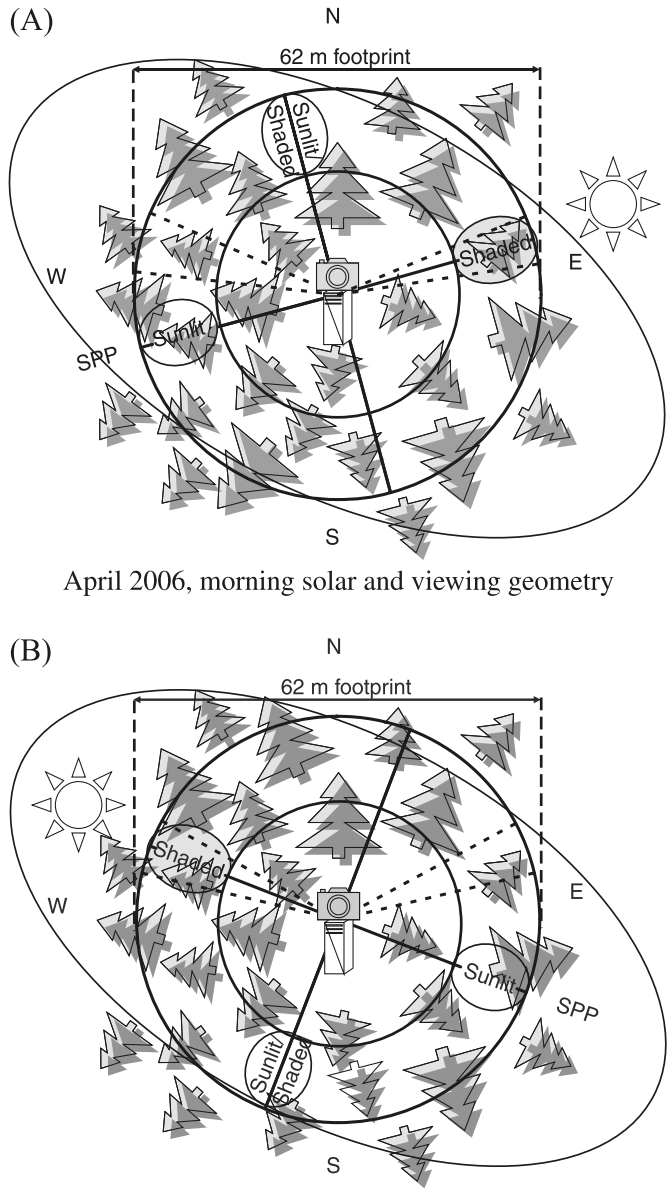

Figure 1. Conceptual representation of the solar and viewing geometries and the regions of the canopy extracted for spectral studies at DF49. A polar coordinate view from above DF49 is centered on the tower. The 360° swath through the Douglas-fir canopy sectors viewed by the AMSPEC falls within the two concentric circles. An ellipse encompassing the site designates a typical fetch for fluxes. The canopy sectors sampled for spectral studies of sunlit, shaded, and shaded–sunlit mix are designated as small ellipses. Examples for the solar principal plane (SPP) are shown in (A) the early morning (~8:30 am in April) and (B) the late afternoon (~4:30 pm in August).

and PAR data, we determined the effective instantaneous LUE in each of these canopy sectors (sunlit, shaded, shaded–sunlit foliage), designated as $LUE_{foliage}$. We also determined the relationship of instantaneous PRI measurements to $LUE_{foliage}$ and examined the change over the growing season, as well as the hypotheses described in the first section of the Introduction.

Materials and methods

Study site

The study site is located in the coastal temperate region of Vancouver Island, British Columbia, Canada, approximately 10 km southwest of the city of Campbell River. The data were collected from a research tower in the Canadian Carbon Program distributed network (49°52′7.8″N, 125°20′6.3″W) and the surrounding second-growth forest at ~300 m above sea level. The forest is dominated by Douglas-fir stands planted in 1949 after harvesting of the original stand (Goodwin, 1937) and therefore is referred to as DF49. It consists of 80% Douglas-fir (*Pseudotsuga menziesii* (Mirbel) Franco), 17% western red cedar (*Thuja plicata* Donn ex D. Don), and 3% western hemlock (*Tsuga heterophylla* (Raf.) Sarg.). The leaf area index (LAI) of this forest was determined to be 7.3 $m^2 \cdot m^{-2}$ (Chen et al., 2006), and that within the tower footprint as 8.4 $m^2 \cdot m^{-2}$ (Humphreys et al., 2006). Seasonal variability was expected to range by 15%–25%, suggesting minimum LAI in winter of 6.3–7.1 $m^2 \cdot m^{-2}$, with the highest seasonal LAI expected in summer, as observed for a nearby young Douglas-fir stand (Humphreys et al., 2006).

The forest is located in the dry maritime Coastal Western Hemlock biogeoclimatic subzone, characterized by a climate with typically cool and dry summers and mild winters (Klinka et al., 1991), with an average annual temperature of 8.6 °C and total annual precipitation of 1450 mm, 75% of which occurs between October and March (Morgenstern et al., 2004). The site was fertilized in 1994 with 200 kg N ha^{-1} applied as urea, although it is one of the most productive forests in Canada (Morgenstern et al., 2004). The soil is a humo-ferric podzol with a gravelly loamy sand texture in the upper 40 cm transitioning to sand with increasing depth and a total soil C content in the upper 1 m of 11.5 kg C m^{-2} (Drewitt et al., 2002; Morgenstern et al., 2004). The lowest soil moisture values have occurred in late summer (August and (or) September) as described by a multiyear dataset (1998–2001, 2003–2005) (Morgenstern et al., 2004; Jassal et al., 2007). The seasonal variability in soil moisture for 2006 was similar to that of previous years (Cheng et al., 2009). A more detailed description of site characteristics can be found in Drewitt et al. (2002).

Year-round eddy covariance flux measurements have been undertaken at DF49 since 1997, and this site has been included in the Canadian Carbon Program (formerly, Fluxnet Canada) network since 2002 (Morgenstern et al., 2004; Margolis et al., 2006).

Data collections from D49 tower

Spectral data were acquired continuously through the 2006 growing season (April through November) with the automated multiangular spectroradiometer for estimation of canopy (AMSPEC) reflectance system. AMSPEC is a fully automated tower-based platform installed at a height of 45 m, or ~10 m above the tree canopy. This system obtained hyperspectral visible–near-infrared (VIS–NIR) reflectance observations (350–1200 nm) using upward- and downward-pointing probes from a Unispec-DC spectroradiometer (PP Systems, Amesbury, Mass.) featuring 256 contiguous bands, although we limited our examination to the 400–900 nm region. Spectra were produced using a 3.5 nm sampling interval, although the actual spectral resolution was ~8 nm at full width half maximum. Both sensors were cross-calibrated manually on a regular basis using a spectralon panel under a range of different sky conditions (Hilker et al., 2007). The measurement error was minimized by (*i*) comparing observations acquired under similar sky conditions only, according to the direct to diffuse ratio; and (*ii*) tracking the PRI measured from the calibration panel throughout the year.

Canopy spectra were acquired from a fixed view zenith angle of 62° to optimize observations for canopy clumping effects (Chen and Black, 1991; Chen, 1996) and a projected canopy instantaneous field of view (FOV) of 20°, an approximate FOV provided as a technical specification (Unispec DC, V1.03, www.ppsystems.com/ApplicationNotes/AN_UniSpec-DC_Accessories.pdf), although the actual area of observation varied slightly with tree height in this homogeneous forest stand (Hilker et al., 2007). Canopy spectra were acquired at a high temporal resolution to capture the spectral dynamics of sunlit and shadowed foliage. The AMSPEC downward-pointing probe was attached to a motor that moved 11.5° to a new position every 30 s and completed a near-360° azimuth sweep of the canopy every 15 min during daylight hours, producing a useable 330° view area around the tower (a 30° range was discarded between 220° and 250° from geodetic north due to obstruction by the tower). Canopy reflectance was computed as the ratio of the canopy radiance acquired from the downward probe to the solar irradiance acquired with the upward-pointing probe equipped with a cosine receptor. Further details about AMSPEC measurements can be found in Hilker et al. (2007).

Half-hour average values have been available year-round since 1997 for eddy covariance flux measurements of CO_2, and sensible and latent heat, from a 45 m tall, 51 cm triangular open-lattice type tower. Net ecosystem exchange (NEE) values were obtained by correcting CO_2 flux measurements for changes in air column storage. Net ecosystem productivity (NEP) values were calculated as –NEE. GPP values were obtained by adding measured daytime NEP values to values of daytime ecosystem respiration (R). The latter were calculated using the exponential relationship between nighttime R measured in sufficiently turbulent conditions (friction velocity > 0.3 $m \cdot s^{-1}$) and soil temperature (T) at the 5 cm depth

(Morgenstern et al., 2004; Black et al., 1996; Goulden et al., 1997). Variability in the dependence of R on temperature (r^2 = 0.75) can be a source of error in this calculation due primarily to underestimation of R during nighttime when turbulent conditions are lacking (Krishnan et al., 2006; 2009). For the occasional gaps in daytime NEP data, GPP values were estimated from fluxes using the rectangular hyperbolic Michaelis–Menton relationship between GPP and PAR (Morgenstern et al., 2004; Jassal et al., 2007). However, variability in the dependence of GPP on incoming radiation (r^2 = 0.62) is one possible error source (Krishnan et al., 2008; 2009), in addition to the <20% error associated with gap-filling using half-hourly data (Humphreys et al., 2006). The solar zenith angle was calculated using the time stamp of each flux measurement (Reda and Andreas, 2004). Estimates of incident and reflected PAR were made from measurements from upward- and downward-looking PAR sensors (model 190 SZ, Li-COR, Lincoln, Nebr.) installed at ~45 m above the ground; these sensors observed an area of the forest stand similar to that of the AMSPEC system, but both sampled a smaller area than that affecting the fluxes. In our analysis, we used half-hourly values of GPP (μmol CO_2 $m^{-2}\cdot s^{-1}$), incident PAR (μmol$\cdot m^{-2}\cdot s^{-1}$), and sensible and latent heat fluxes ($W\cdot m^{-2}$) and calculated the bulk canopy LUE as GPP/PAR (μmol CO_2 MJ^{-1} PAR), even though GPP and PAR represent values associated with slightly different areas centered on the tower.

Canopy structure to derive sunlit versus shadowed canopy

The proportion of shaded to sunlit tree crowns was estimated using a canopy surface model derived from airborne scanning light detection and ranging (lidar) observations. Lidar data with a footprint of 0.19 m were acquired at the site on 8 June 2004 by Terra Remote Sensing (Sidney, B.C.) from a Bell 206 Jet Ranger helicopter. Separation of vegetation and terrain was carried out using specialized software (Terrascan v. 4.006; Terrasolid, Helsinki, Finland), resulting in a forest surface topography map of the site, from which a three-dimensional canopy surface model of the forest canopy structure was generated for a 1 km circular eddy covariance footprint (Hilker et al., 2008a; 2008b; 2008c). The shadow fractions at half-hour intervals were simulated using the canopy surface model and a hill-shade algorithm (Van Den Eeckhaut et al., 2005) (ArcGIS 9.1, ESRI Inc., Redlands, Calif.) for each 11.5° canopy azimuth sector of DF49 viewed with AMSPEC at various BRDF combinations of sun and view geometries. For each time period, a 256 gray-scale raster of the same size and resolution as the input canopy surface model was generated to represent the illumination conditions at each canopy sector (i.e., azimuth interval). Threshold values were employed to assign each canopy sector into sunlit, shaded, or intermediate illumination conditions (Hilker et al., 2008a; 2008b; 2008c). We refer to these dynamic canopy sectors, which shift in time and under different sky conditions, as "sunlit foliage," "shaded foliage," and mixed "intermediate (shaded–sunlit) foliage" (**Figure 1**). The fraction of each foliage sector per half-hour measurement period (April–November) was determined by summing the number of pixels assigned to each of the three classes and dividing by the total raster size. A validation of this method was previously performed by Hilker et al. (2007; 2008a; 2008b; 2008c).

Spectral data processing

Several spectral bioindicator reflectance indices were derived from the directional reflectance spectra at each measurement period per canopy foliage group: sunlit, shaded, and shaded–sunlit. The three PRI variations (PRI_{570}, PRI_{551}, and PRI_{488}) were calculated using the physiologically active response at 531 nm and one of three reference bands (570, 551, and 488 nm) in the form of normalized difference indices (Equation (2)). The normalized difference vegetation index (NDVI) (Tucker, 1979; Huete et al., 2002) was derived using red (655 nm) and near-infrared (NIR, 865 nm) bands as NDVI = (ρNIR – ρred)/(ρNIR + ρred), and the enhanced vegetation index (EVI) was calculated using these bands plus a blue band (460 nm) as EVI = 2.5[(ρNIR – ρred)/(1 + ρNIR + 6.0ρred – 7.5ρblue)] (Huete et al., 1994; 2002).

To investigate diurnal and seasonal changes of these spectral indices under different sun and view angle conditions, the following preprocessing steps were applied. First, several representative sunny and overcast (e.g., cloudy) days were selected from each month (April–November 2006), and the corresponding spectral and tower flux data were extracted from the continuous DF49 database. Spectral measurements from those days were subdivided into the three canopy sectors (sunlit, shaded, or shaded–sunlit) according to the relative azimuth angle, the angle between the sensor, and the solar positions. The dynamic sunlit foliage sector of the canopy was defined as those spectra acquired when the relative azimuth angle was 180 ± 10° (e.g., the azimuth region of the BRDF hotspot), and the shaded foliage sector was defined for those spectra acquired when the relative azimuth angle was centered on 0° (e.g., the azimuth region of the BRDF darkspot). The intermediate (shaded–sunlit) canopy sector was retrieved in a plane perpendicular to the SPP where the relative azimuth angle region sampled was 90 ± 10°.

To examine the overall seasonal behavior of a PRI index associated with the three canopy foliage groups (sunlit, shaded, intermediate), PRI_{570} was retrieved on several days each month at three times of the day local time (8:30 am ± 15 min, 12:15 pm ± 15 min, and 4:30 pm ± 15 min), producing nine PRI courses (three foliage groups × three times of the day) spanning the 2006 season. Seasonal averages for the PRI_{570} at these three times of day per foliage group were also examined for sunny versus overcast (highly diffuse) days. The diurnal courses for spectral indices (PRI_{570}, PRI_{488}, PRI_{551}, NDVI, and EVI) associated with the three canopy foliage groups were examined for sunny versus cloudy days, in terms of local time of day and solar zenith angle (SZA), in 2 months when combined

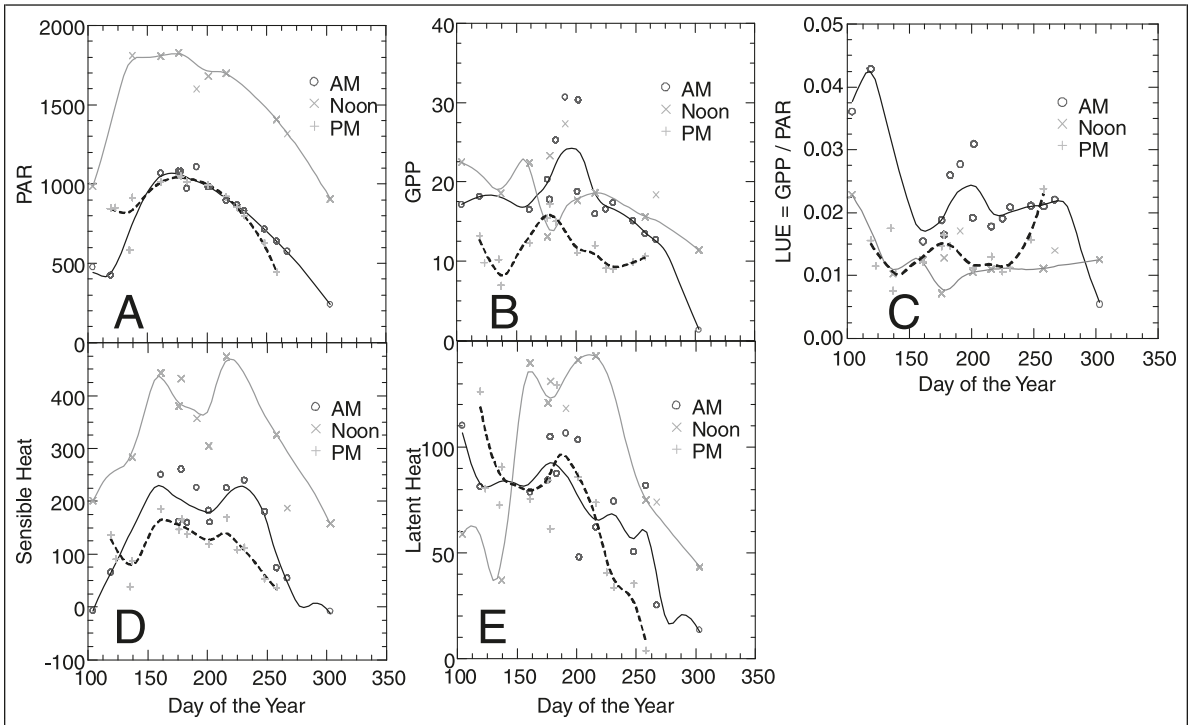

Figure 2. Average seasonal courses for tower measurements at DF49 for several fluxes in the morning (8:30 am PST), noon (12:15 pm PST), and afternoon (4:30 pm PST): (A) PAR ($\mu mol \cdot m^{-2} \cdot s^{-1}$); (B) GPP ($\mu mol\ CO_2\ m^{-2} \cdot s^{-1}$); (C) LUE ($\mu mol\ CO_2\ \mu mol^{-1}$ PAR); (D) sensible heat ($W \cdot m^{-2}$); (E) latent heat ($W \cdot m^{-2}$). ○ and black line, morning; × and gray line, noon; + and broken line, afternoon.

environmental stresses were assumed to be relatively low (April) versus high (August).

In addition to the bulk canopy LUE computed directly from the above-canopy eddy covariance fluxes, we estimated the dynamic within-canopy LUE of the three foliage groups. We assumed that the total (direct + diffuse) received in each canopy foliage sector could be scaled from the top-of-canopy PAR according to its modeled shadow fraction. Therefore, we calculated the instantaneous APAR per sector as the product of the shadow fraction (S, $0 \rightarrow 1$, $S \neq 1$), the top of canopy PAR, and the NDVI (>0, between 0 and 1) as a surrogate for f_{APAR} (Goward and Huemmrich, 1992; Huemmrich, 2001), which was obtained from the AMSPEC spectra, as

$$APAR = PAR(1 - S)NDVI \quad (3)$$

Next, we utilized the rectangular hyperbolic relationship (from traditional CO_2 light response curves) between GPP and PAR that describes the photosynthetic light curve potential for foliage at this forest (Humphreys et al., 2006; Morgenstern et al., 2004) to estimate the net instantaneous photosynthetic capacity (P_n) in each foliage group as

$$P_n = \frac{\alpha P_\infty (PAR)}{\alpha (PAR) + P_\infty} \quad (4)$$

where P_∞ is the maximum value of P_n at high PAR, and α is the effective quantum yield. LUE per foliage group at each available measurement ($LUE_{foliage}$) was calculated as the ratio of Equation (4) to Equation (3), i.e., P_n/APAR. Regression relationships across the full season on clear sky (sunny) days were developed for the three PRI indices versus $LUE_{foliage}$. In addition, the monthly variation in $LUE_{foliage}$ across the season (April–November) was examined per foliage group. Statistical analyses were performed using Systat V.11 (Jandel Scientific, San Rafael, Calif.).

Results

Canopy tower flux measurements

The seasonal courses for bulk canopy fluxes measured at the DF49 tower under clear sky conditions in 2006, based on our sunny day sample set, are shown for three times of day, namely morning (8:30 am), noon, and afternoon (4:30 pm), for variables used to calculate LUE or expected to influence LUE (**Figure 2**): PAR ($\mu mol \cdot m^{-2} \cdot s^{-1}$), GPP ($\mu mol\ CO_2\ m^{-2} \cdot s^{-1}$), LUE ($\mu mol\ CO_2\ \mu mol^{-1}$ PAR), sensible heat ($W \cdot m^{-2}$), and latent heat ($W \cdot m^{-2}$). All of these fluxes show considerable diurnal and seasonal variations. The two most similar flux courses are PAR and sensible heat (**Figures 2A**, **2D**), exhibiting relatively smooth seasonal responses at each time of day examined, and with noontime fluxes substantially higher than those in the mornings and afternoons. Sensible heat also displayed seasonal peaks in June and August at each time of day examined, whereas the corresponding double peaks for latent heat flux in

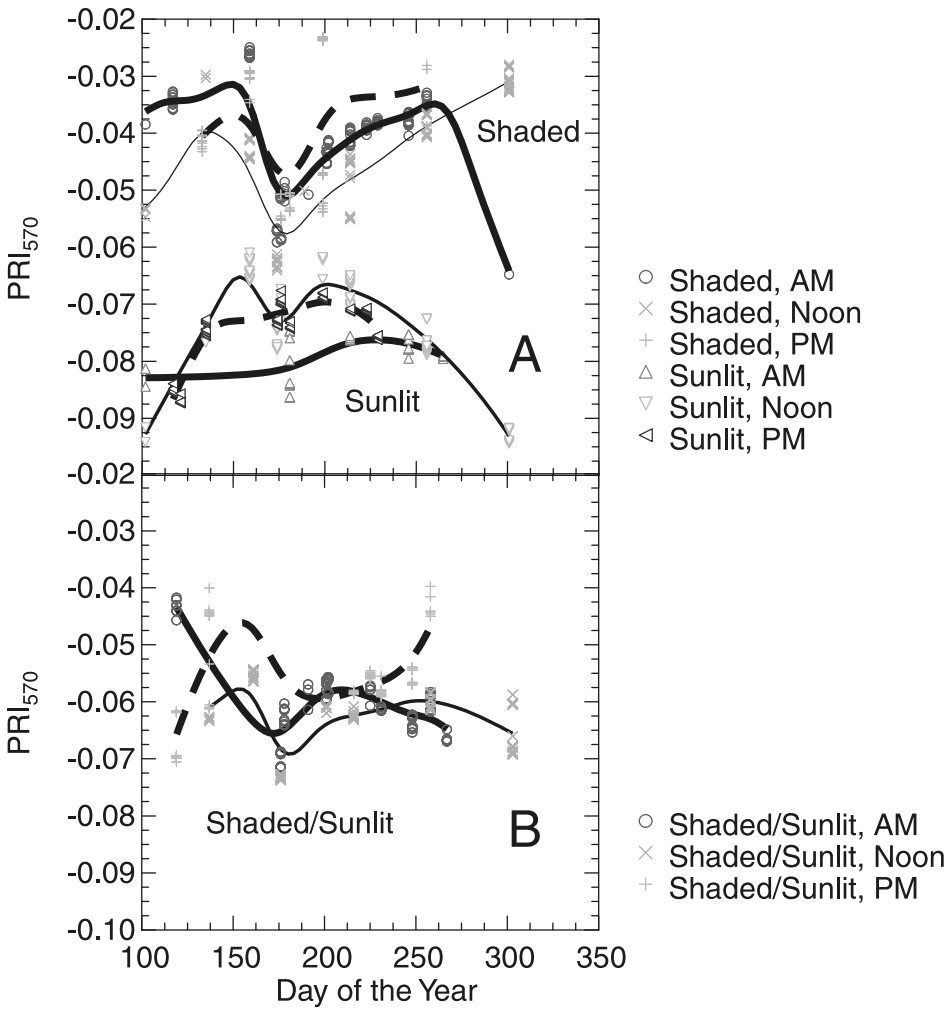

Figure 3. Seasonal courses for PRI_{570} from spectra acquired on sunny days during 2006 with the AMSPEC system from the DF49 tower. The different curves show PRI_{570} for three canopy foliage sectors (shaded, shaded–sunlit, sunlit) measured in the morning (~8:30 am PST), near noon (~12:30 pm PST), and in the afternoon (~4:30 pm PST): (A) shaded canopy and sunlit canopy sectors; (B) mixed shaded–sunlit canopy sector. Thick black lines indicate the morning courses, and broken black lines indicate the afternoon courses for each of the three foliage groups in (A) and (B). Noontime courses are designated with a gray line. Note that trend lines were made with the distance weighted least square (DWLS) method in Systat V.11 with the tension parameter set to 0.5, fitted within the data range.

June and August only occurred at midday (**Figure 2E**). Although GPP seasonal courses overlapped at these three times of day, the morning GPP was highest in July and tracked latent heat throughout the season (**Figure 2B**). Bulk canopy LUE (**Figure 2C**) exhibited higher values in the morning, especially in the springtime.

Canopy AMSPEC measurements: seasonal PRI_{570} averages per foliage sector

The diurnal variation in PRI_{570} on sunny days across the 2006 season (April–November) observed from the tower's AMSPEC system was more complex than that for the bulk canopy fluxes shown in **Figure 2**, for each of the three canopy foliage groups (**Figure 3**). The spectral responses for shaded versus sunlit foliage were distinctly different on sunny days. In general, shaded foliage maintained the highest PRI_{570}, and sunlit foliage the lowest PRI_{570} (**Figure 3A**, upper versus lower line sets), with the values for the intermediate shaded–sunlit group falling between (**Figure 3B**). In addition, there was a notable drop in PRI_{570} values around the summer solstice, clearly attributable to high light stress, which was evident throughout the day in the shaded sector and at midday for sunlit and mixed sectors (**Figure 3**).

Comparisons among the canopy sectors (**Figure 4**) were also made for daily averages on both sunny and overcast days across the season (**Figures 4A**, **4B**) and for seasonal averages at three times of day (**Figures 4C**, **4D**). For sunny days, the PRI_{570}

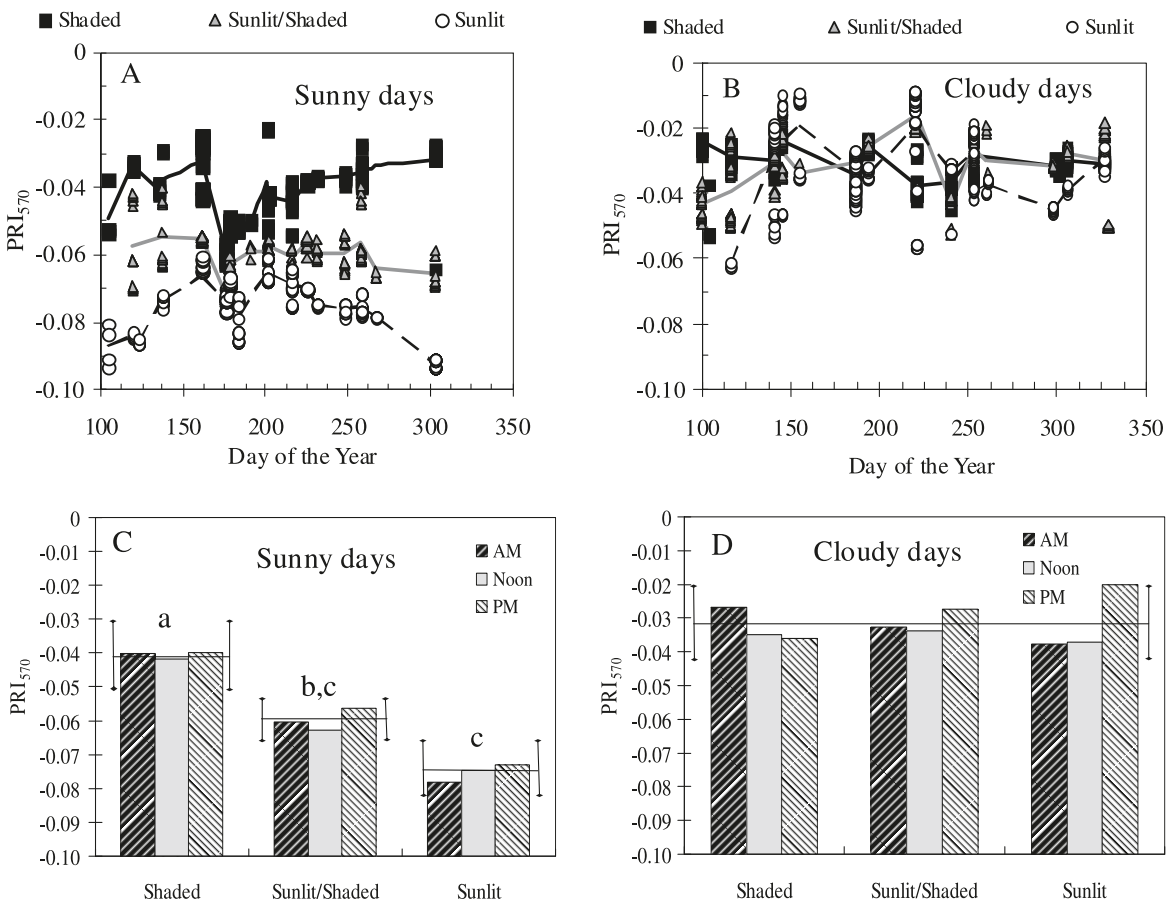

Figure 4. Seasonal courses (April–November) for daily averages of PRI_{570} are shown for three foliage groups (shaded, intermediate sunlit–shaded, and sunlit) at the Douglas-fir stand: (A) sunny days; (B) cloudy days. For each foliage group, the seasonal PRI_{570} averages at three times of day (morning, noon, and afternoon) are shown: (C) sunny days, where the mean ± SD per foliage group is indicated with horizontal and vertical bars; (D) cloudy days, where a single mean ± SD is given for all foliage. On sunny days (C), the seasonally averaged PRI_{570} values for the three foliage groups displayed significant diurnal differences, summarized here with the mean ± SE (n, SD, COV): shaded foliage, –0.04 ± 0.001 (n = 294, SD = 0.010, COV = 24.8%); sunlit foliage, –0.075 ± 0.001 (n = 262, SD = 0.008, COV = 11.0%); and shaded/sunlit foliage, –0.060 ± 0.000 (n = 266, SD = 0.007, COV = 11.6%). On cloudy days (D), no foliage group differences for PRI_{570} were significant across the season (mean ± SE: –0.0315 ± 0.00034; n = 926, SD = 0.010, COV = 32.8%).

differences among foliage groups were maintained (shaded > sunlit–shaded > sunlit) when multiple observations per day were combined to yield daily PRI_{570} averages (**Figure 4A**). Even when averaged over the growing season (**Figure 4C**), this trend on sunny days was maintained ($\bar{X}$ ± SE: shaded, –0.04 ± 0.001 > shaded/sunlit, –0.06 ± 0.0004 > sunlit, –0.075 ± 0.001). However, these distinctions among foliage groups disappeared on overcast days (**Figure 4B**) when excess light conditions did not occur and which yielded higher and relatively constant PRI_{570} values seasonally (–0.032 ± 0.0003, **Figure 4D**) across all three canopy sectors. In fact, this average PRI_{570} on highly diffuse radiation days is approximately twice the average value observed on sunny days (–0.06 ± 0.03). A reversal to a constant, high PRI value for the canopy as a whole on cloudy (or highly diffuse radiation) days reveals that the high light-induced PRI reductions seen on intermittent sunny days were fully ameliorated on days having more favorable lower light intensities (and related lower temperatures). Further examination of **Figures 4C** and **4D** reveals that sunlit leaves generally exhibited recovery in the late afternoons from light-induced photosynthetic down-regulation, as captured by higher late afternoon PRI_{570} values on both sunny and overcast days.

Canopy AMSPEC measurements: diurnal PRI_{570} responses

The diurnal changes in PRI_{570} on sunny and overcast days were further examined for a larger set of observations acquired throughout each day (not limited to three times of day) in 2 months (April and August) (**Figure 5**). The diurnal

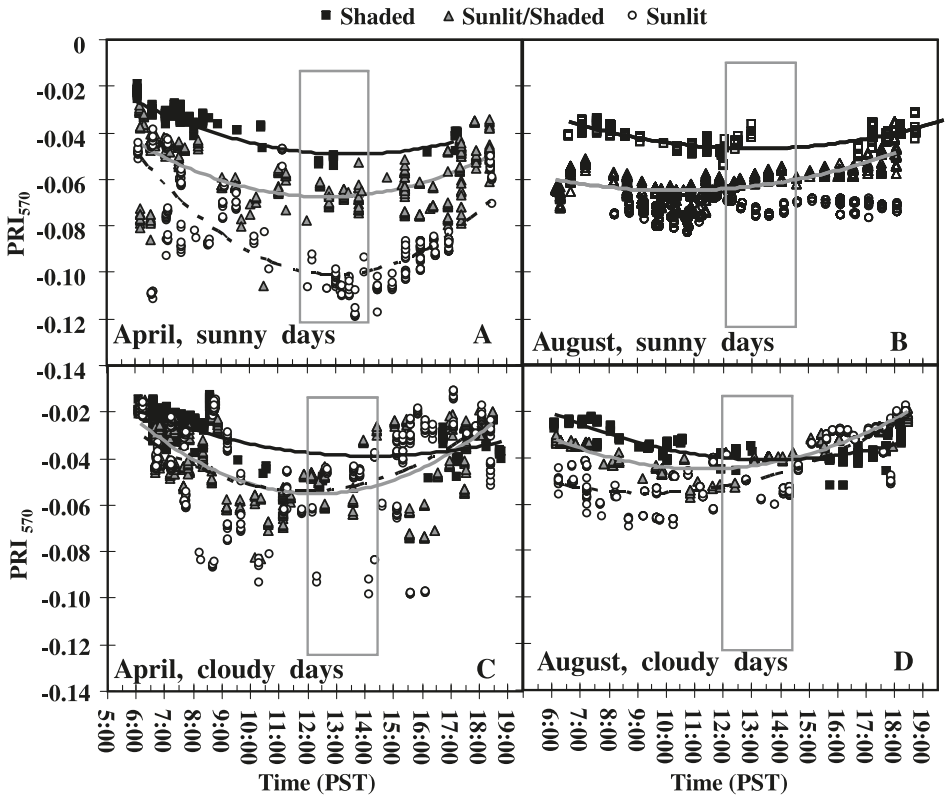

Figure 5. Diurnal PRI_{570} courses for the three foliage groups are shown relative to local time (PST) for sunny and cloudy days in April and August: (A) April, sunny days; (B) August, sunny days; (C) April, cloudy days; (D) August, cloudy days. The midday period is designated with a rectangle in each panel. Shaded foliage is shown with solid black lines, sunlit foliage with broken black lines, and shaded–sunlit foliage with solid gray lines. All other symbols and line types as defined in **Figure 4**.

differences among the three groups were more pronounced for sunny days in April, especially at midday when the lowest PRI_{570} values were observed (**Figure 5A**), whereas diurnal effects were suppressed on sunny August days (**Figure 5B**). Since the early morning and late afternoon PRI_{570} values were similar in April and August, the primary seasonal difference between these 2 months was the reduced down-regulation (i.e., higher PRI_{570} values) at midday producing flatter diurnal curves in August. The PRI_{570} for shaded foliage had significantly higher sunny day values than the other two groups in both April and August (**Figures 5A**, **5B**). The corresponding April–August diurnal courses for overcast days (**Figures 5C**, **5D**) exhibited fewer distinctions among foliage groups, as observed previously. For the sunlit canopy foliage sector, PRI_{570} values were generally higher on cloudy days than on sunny days (e.g., **Figure 5C** versus **Figure 5A**), as might be expected when conditions favored lower light stress.

When these data were plotted against SZA, a proxy for general environmental conditions associated with irradiance and temperature conditions, positive linear relationships for PRI_{570} versus SZA emerged (**Figure 6**). On sunny April days, the strongest PRI_{570} dependence on SZA (r^2 = 0.56) was displayed by the sunlit foliage (**Figure 6A**). For April sunny days combined over all foliage groups, SZA explained 78% of the variation in PRI_{570} (P < 0.0001, n = 834). However, on sunny August days (**Figure 6B**), the shaded foliage was the only group to display PRI_{570} dependence on SZA (r^2 = 0.65), possibly because this group maintained sufficient tissue water in the shade. For cloudy days (**Figures 6C**, **6D**), the overall dependence of PRI_{570} on SZA was low in both months (April, r^2 = 0.31; August, r^2 = 0.29), but the high PRI_{570} values associated with shaded foliage were maintained. In all cases, the highest PRI_{570} values occurred for large SZAs (early and late in the day), indicating reduced physiological stress under lower PAR intensities. When sunny day data from all months (April–November) were combined, SZA explained 52% of the variation in PRI_{570} (P < 0.0001, n = 9660) across foliage groups (data not shown). This is additional evidence that the PRI responses were correlated with light intensity and the associated temperature levels (e.g., sensible heat).

For comparison with PRI indices that can be computed using MODIS ocean band data (Drolet et al., 2005; 2008a), two other PRI indices (PRI_{488} and PRI_{551}) were examined using the sunny days in April (**Figure 7**; n = 834). PRI_{551} gave diurnal trends similar to those of the original PRI_{570} for the three foliage groups (combined r^2 = 0.86, P < 0.0001). However, PRI_{488}

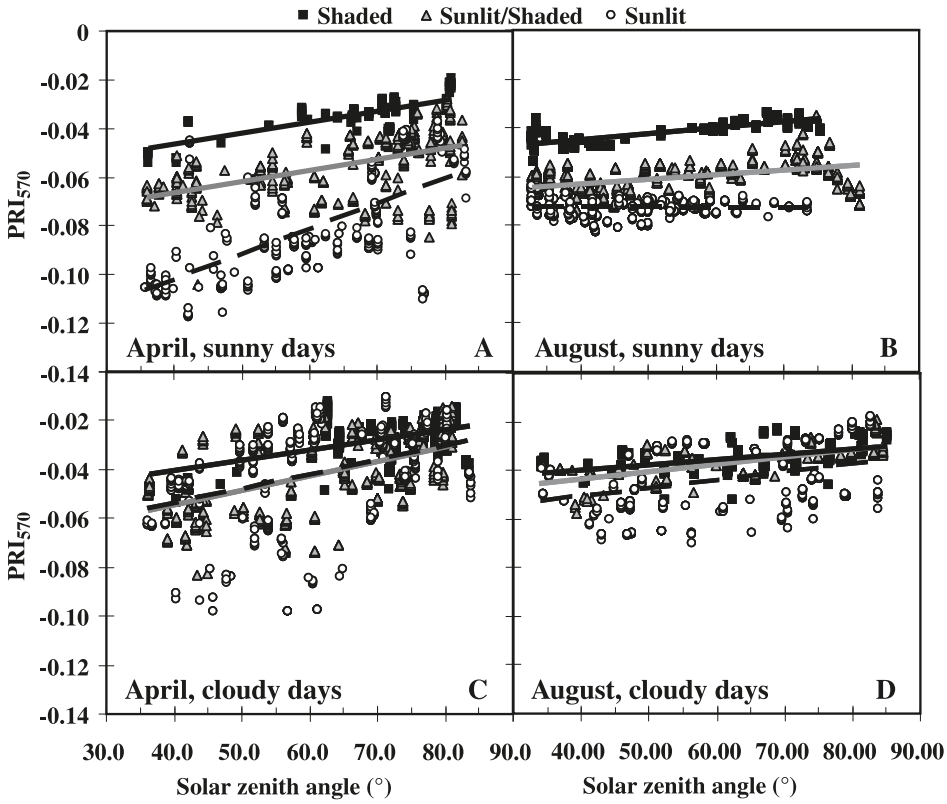

Figure 6. Diurnal PRI_{570} courses for the three foliage groups are shown relative to solar zenith angle (SZA) for sunny and cloudy days in April and August. Symbols and line types as defined in **Figure 5**. Relevant statistics for foliage groups are summarized as follows: (A) sunny days in April, $PRI_{570(sunlit)} = -0.14360 + 0.00104SZA$ ($n = 317$, $r^2 = 0.43$, $P < 0.0001$), $PRI_{570(mixed)} = -0.08450 + 0.00046SZA$ ($n = 386$, $r^2 = 0.27$, $P < 0.0001$), and $PRI_{570(shaded)} = -0.06577 + 0.00046SZA$ ($n = 131$, $r^2 = 0.56$, $P < 0.0001$); (B) sunny days in August, $PRI_{570(sunlit)} = -0.07211 - 0.00001SZA$ ($n = 483$, $r^2 = 0.07$, $P < 0.003$), $PRI_{570(mixed)} = -0.07031 + 0.00018SZA$ ($n = 566$, $r^2 = 0.17$, $P < 0.0001$), and $PRI_{570(shaded)} = -0.05496 + 0.00024SZA$ ($n = 276$, $r^2 = 0.65$, $P < 0.0001$); (C) cloudy days in April ($n = 1088$, combined $r^2 = 0.31$, $P < 0.0001$); (D) cloudy days in August ($n = 788$, combined $r^2 = 0.29$, $P < 0.0001$).

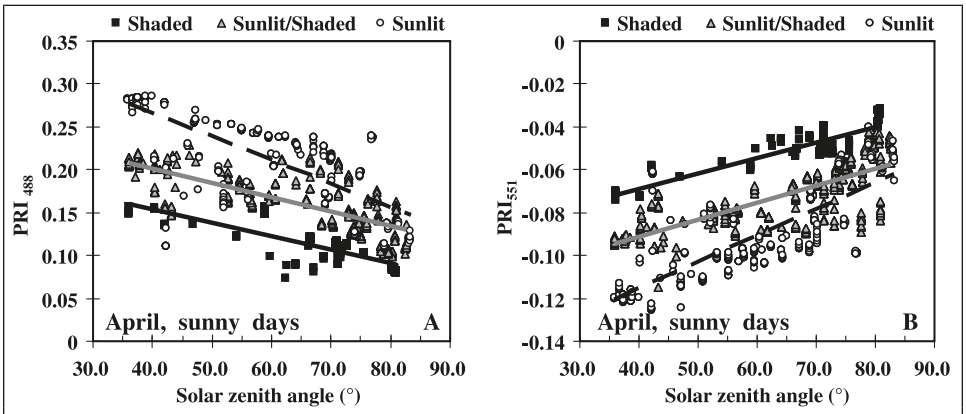

Figure 7. Diurnal courses on sunny days in April ($n = 834$) for two additional PRI indices are shown relative to SZA for the three foliage groups: (A) PRI_{488} (combined $r^2 = 0.70$, $P < 0.0001$); (B) PRI_{551} (combined $r^2 = 0.86$, $P < 0.0001$).

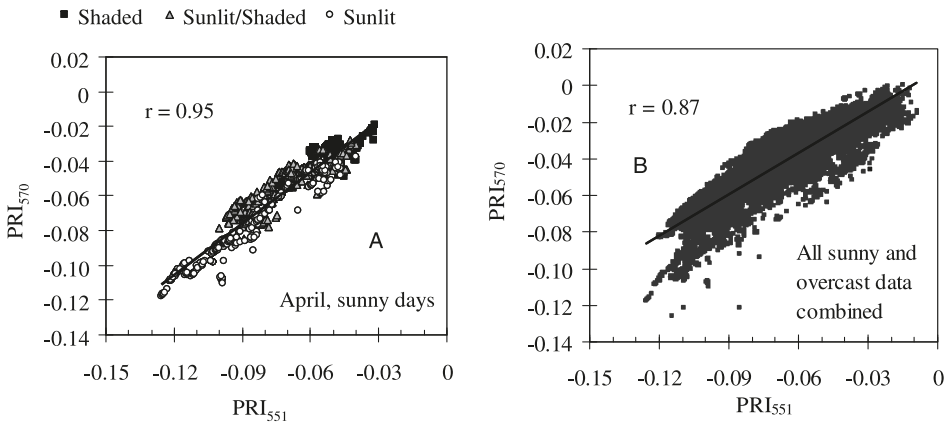

Figure 8. Correlation between PRI_{570} and PRI_{551}: (A) sunny days in April (r = 0.95, n = 834, P < 0.000); (B) all data for sunny and cloudy days combined, April–November (r = 0.87, n = 17 821, P < 0.000).

displayed an inverse relationship to SZA, for which the higher values were associated with the sunlit foliage, and the overall dependence on SZA was slightly lower (combined r^2 = 0.70, P < 0.0001). For our 2006 dataset, values for PRI_{551} were always negative, whereas values for PRI_{488} were always positive, with the PRI values for the least light stressed foliage approaching zero in both cases. PRI_{551} and PRI_{488} were strongly correlated (r = 0.93), as were PRI_{570} and PRI_{551} (r = 0.95, P < 0.000) (**Figure 8A**); the latter correlation retained separation of the shaded–mixed foliage from the sunlit foliage, arranged on opposite sides of the regression line. When data from sunny and overcast days over the entire season were combined, this strong correlation between PRI_{570} and PRI_{551} was still maintained (r = 0.87, **Figure 8B**). Furthermore, when the AMSPEC data (originally acquired at a 3.5 nm spectral sampling interval) were averaged over three adjacent channels to provide 10 nm spectral bins, we produced bands comparable to the MODIS bands: PRI_{570} (with 3.5 nm sampling interval) and PRI_{570} (10 nm resolution) were almost perfectly correlated for sunny days (r = 0.999, n = 9660, root mean square error (RMSE) = 0.0017) and for overcast days (r = 0.993, n = 8161, RMSE = 0.0014). However, a superior result was obtained for PRI_{551}, for which a similar correlation at two band widths (3.5 nm versus 10 nm) was attained with about half the measurement error obtained with PRI_{570} (sunny days: r = 0.999, RMSE = 0.0007; cloudy days: r = 0.999, RMSE = 0.0008). This supports the use of 10 nm wide spectral bands, and either PRI_{570} or PRI_{551} to monitor change over time.

For comparison with PRI indices, the NDVI and EVI as a function of SZA on sunny days in April and August are also presented (**Figure 9**). There were no statistically significant differences among foliage groups for NDVI in either month (**Figures 9A**, **9B**). The NDVI in April declined linearly (r^2 = 0.60) from the highest values at midday (~0.78) to 0.42 at large SZA, with greater similarity to the behavior of PRI_{488} (**Figure 7A**). However, the NDVI in August was relatively constant throughout the day and higher in value (0.78–0.85), apparently associated with a somewhat higher midsummer LAI, in agreement with field-measured LAI (Humphreys et al., 2006), that was capable of sustaining constant PAR interception throughout the day (also refer to **Figure 10C**). In the following sections, we used the NDVI acquired with the AMSPEC system as a surrogate for f_{APAR} at each measurement set (Goward and Huemmrich, 1992; Huemmrich, 2001). In contrast to the behavior of the NDVI, EVI values for sunlit foliage in August were clearly distinct from and significantly higher than (ranging from 0.5 to 1.1) those for the other two groups (**Figure 9D**) and exhibited a strong positive linear relationship with SZA (r^2 = 0.87; **Figure 9D**). In April, the EVI for sunlit foliage during the afternoon was linearly related to SZA, whereas the morning EVI values for sunlit foliage were substantially lower and unrelated to SZA, and similar to the responses of the mixed shaded–sunlit group (**Figure 9C**). The higher EVI values for sunlit foliage demonstrate greater photosynthetic down-regulation (i.e., high light-induced responses), which emerges due to the EVI band weighting factors, which accentuate the reflectance contributions of the visible bands relative to the NIR.

Estimating the dynamic LUE per foliage sector

The shadow fraction, which was modeled using lidar data, was logarithm-linearly related to the PRI_{570} (**Figure 10A**), for which an example is provided from August (r^2 = 0.82, n = 1325). The shadow fraction for the three foliage groups displayed both diurnal and seasonal differences (**Figure 10B**). We used this shadow fraction information in conjunction with the above-canopy PAR (direct + diffuse), and NDVI values (as a surrogate for f_{APAR}), to estimate APAR available for photosynthesis in each of these groups. APAR per foliage group also displayed diurnal and seasonal variations (**Figure 10C**). $LUE_{foliage}$ for each group on sunny days throughout the season ($(P_n/APAR)_{foliage}$) from Equations (3)

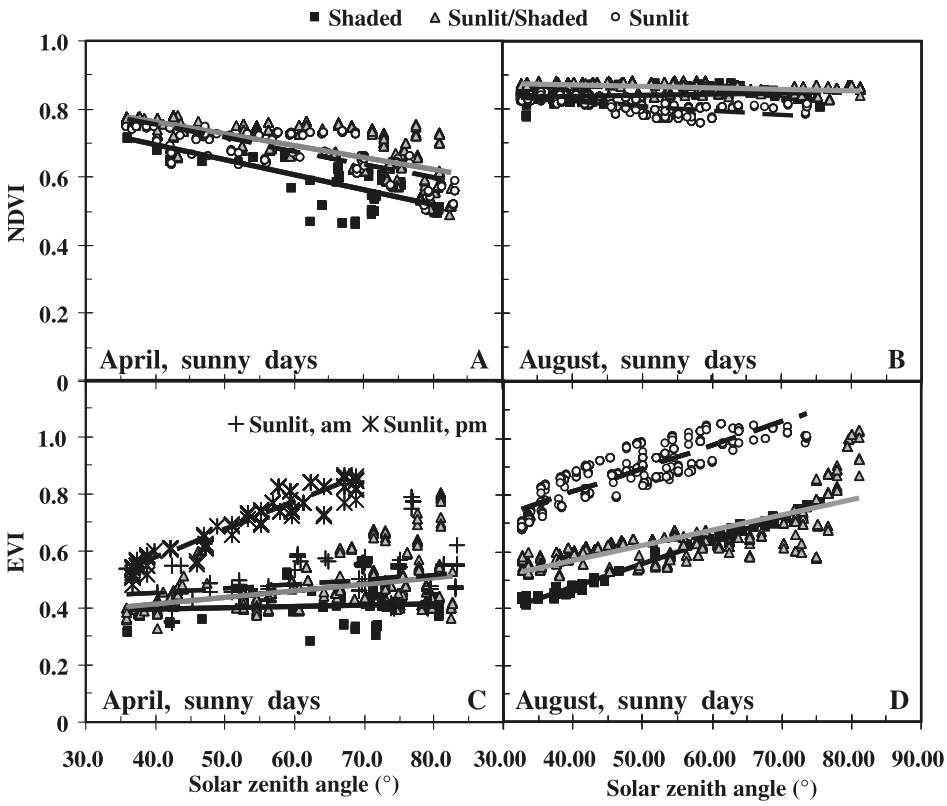

Figure 9. Diurnal courses on sunny days for two vegetation indices (NDVI, EVI) for the foliage groups are shown relative to SZA in April and August: (A) NDVI in April for three foliage groups (n = 834, combined r^2 = 0.60, P < 0.0001); (B) NDVI in August (n = 1325, no relationship); (C) EVI in April, where shaded foliage displays different behavior in the afternoon than in the morning and midday, requiring four foliage groups (n = 834, r^2 = 0.58, P < 0.0001); (D) EVI in August for three foliage groups (n = 1325, combined r^2 = 0.88, P < 0.0001). Symbols and line types as defined in **Figure 4** except for (C), where sunlit foliage is divided into two groups, namely morning through midday (○) and afternoon (*).

and (4) yielded values that ranged between 0.012 and 0.078 µmol C µmol^{-1} APAR (**Figure 11**).

This effort to estimate the effective LUE of the foliage in each sector ($LUE_{foliage}$), rather than to rely only on the tower-acquired bulk canopy LUE, enabled us to demonstrate that each of the three PRI indices on sunny days was linearly related to $LUE_{foliage}$ over the season (n = 822; **Figure 11**). However, there was a 21% difference among these indices in the variance explained by PRI: for the traditional PRI_{570}, r^2 = 0.59 (P < 0.0001, **Figure 11A**); for PRI_{551}, a substantially higher correspondence was attained, with r^2 = 0.80 (P < 0.0001, **Figure 11B**); and for PRI_{488}, an intermediate result was obtained, with r^2 = 0.72 (P < 0.0001, **Figure 11C**). We should point out that an important foliage group was not included in this study, namely the foliage in deep shade that could not be directly viewed by the AMSPEC. AMSPEC continuously viewed the foliage of the outer branches of trees under dynamic light conditions. Consequently, no PRI observations were made of foliage associated with deep shade, located on branches within the tree interior. From examination of **Figure 11B**, we might speculate that the relationship continues to be linear at higher values, such that the deeply shaded foliage sector might have generated PRI_{551} values between –0.04 and zero associated with the highest $LUE_{foliage}$ values, ≥0.065 µmol C µmol^{-1} APAR. However, we cannot know from these data whether the relationship remains linear or asymptotes beyond the measured ranges, as conceptualized in **Figure 12**. Nevertheless, it should be possible in the future to account for this foliage sector and include it in canopy LUE assessments. We offer this idea because there may be unexplored consequences for the LUE of the entire canopy that result from the integrated, relative contributions from all foliage distributed throughout the canopy, whose average and instantaneous light environments are related to plant and canopy structure, stand density, and LAI. This may be especially true for interpreting "ground truth" obtained with oblique views acquired from above or from ground-based measurements made below or from the side of the canopy which might capture larger contributions from the deeply shaded foliage.

The variable success in relating PRIs to $LUE_{foliage}$ led us to question whether or not the optimal PRI indices had been

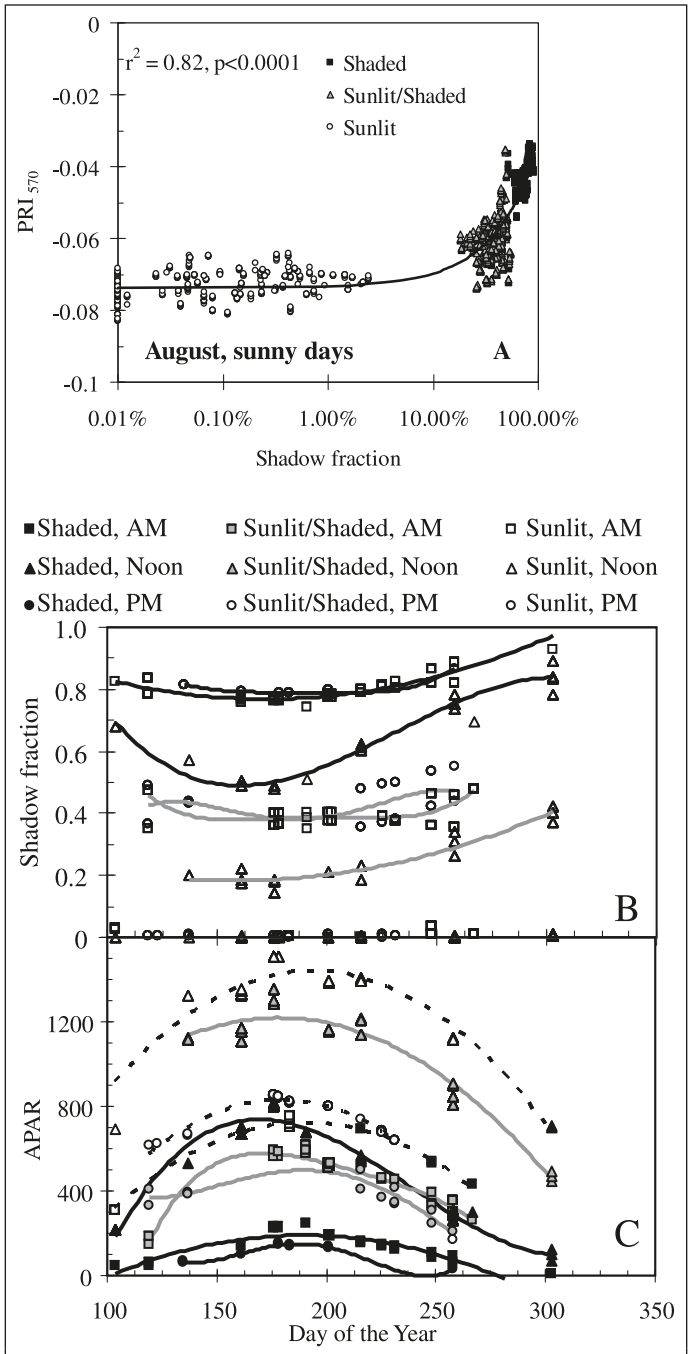

Figure 10. The shadow fraction, as modeled from lidar data, for the three foliage groups is examined on sunny days: (A) in relation to changes in PRI_{570} in August ($r^2 = 0.82$, $n = 1325$, $P < 0.0001$); (B) throughout the 2006 growing season (April–November, $n = 822$) at three times of day; (C) when utilized to estimate APAR, as (1 – shadow fraction)NDVI × $PAR_{top\ of\ canopy}$.

identified for sunny days when high light-induced photosynthetic down-regulation was potentially occurring. Therefore, we examined the correlation to LUE of all possible narrow band PRI indices (using the 3.5 nm sampling interval) on sunny days across the entire growing season ($n = 822$) for LUE presented in three different formulations: $LUE_{foliage}$, LUE_{tower}, and LUE_{canopy} (**Figure 13**). All possible PRI indices were computed for a fixed physiologically active band at 531 nm, but with the reference band varied (400–900 nm). $LUE_{foliage}$ exhibited strong positive correlations with PRI computed with reference wavelengths in the green region between ~540 and 575 nm ($r \approx 0.90$) or in the far-red (~710 nm, $r \approx 0.65$). $LUE_{foliage}$ exhibited strong negative correlations with PRI when computed with reference wavelengths in the far-blue (~480–515 nm, $r \approx -0.85$) or red (670–680 nm, $r \approx -0.80$) regions. The two bulk canopy LUE estimates were not strongly correlated with PRI, although weak positive correlations were obtained for PRI when computed with a green reference band close to 570 nm ($r \approx 0.20$). This analysis shows that we have in fact identified the three most useful PRI indices. Further review of the reflectance variability of individual narrow bands (e.g., R_{488}, R_{531}, R_{551}, R_{570}, R_{678}, R_{800}) over the study's sunny day seasonal dataset revealed that the percent coefficient of variation (%COV) per band ranged between 50% and 63%. R_{531} and R_{551} had the lowest seasonal %COV overall, at 50.4% and 50.9%, respectively.

The seasonal reflectance variability was substantially higher for shaded foliage in all bands (except R_{800}): %COV for R_{531} and R_{551} in shaded foliage was 42%–46% versus 28% in sunlit foliage, and only 17%–18% for the mixed (shaded–sunlit) group. This shows that reflectance in the PRI wavelengths for sunlit leaves, receiving primarily direct radiation at the highest available intensities, was much more uniform than that for shaded leaves, which received more variable and higher diffuse radiation. Consequently, the range of PRI_{570} values related to $LUE_{foliage}$ for shaded foliage (–0.02 to –0.07) was greater than that for sunlit leaves (–0.65 to –0.95) (refer to **Figure 11A**).

Examining the seasonality of $LUE_{foliage}$

The seasonal courses of $LUE_{foliage}$ for the three foliage groups at three times of day are shown for the 2006 growing season (April–November, **Figure 14**). For $LUE_{foliage}$ of shaded foliage, a seasonal bowl shape in mornings–afternoons is evident (top two curves), but the midseason depression is much shorter (~20 days) than that for other groups (40–70 days). $LUE_{foliage}$ for shaded foliage at noon was lower and similar to that for morning–afternoon courses for the mixed and sunlit groups. The lowest and flattest seasonal responses were produced at noontime for the sunlit and mixed foliage groups (bottom two curves in **Figure 14**). We then examined the average $LUE_{foliage}$ values ($\bar{X}$ ± SE) for sunny days in each month (April–October) at midday versus daily averages (**Figure 15**), providing further evidence of the seasonal variability of this parameter. A decline in daily $LUE_{foliage}$ (**Figure 15B**) over the three foliage groups (shaded > mixed > sunlit) is apparent across the 2006 season, with the monthly means ranging between 0.015 μmol C μmol^{-1} APAR (for sunlit foliage in June) and 0.058 μmol C μmol^{-1} APAR (for shaded foliage in April–May). The bowl-shaped $LUE_{foliage}$ monthly time courses (**Figures 14, 15**), centered around the summer

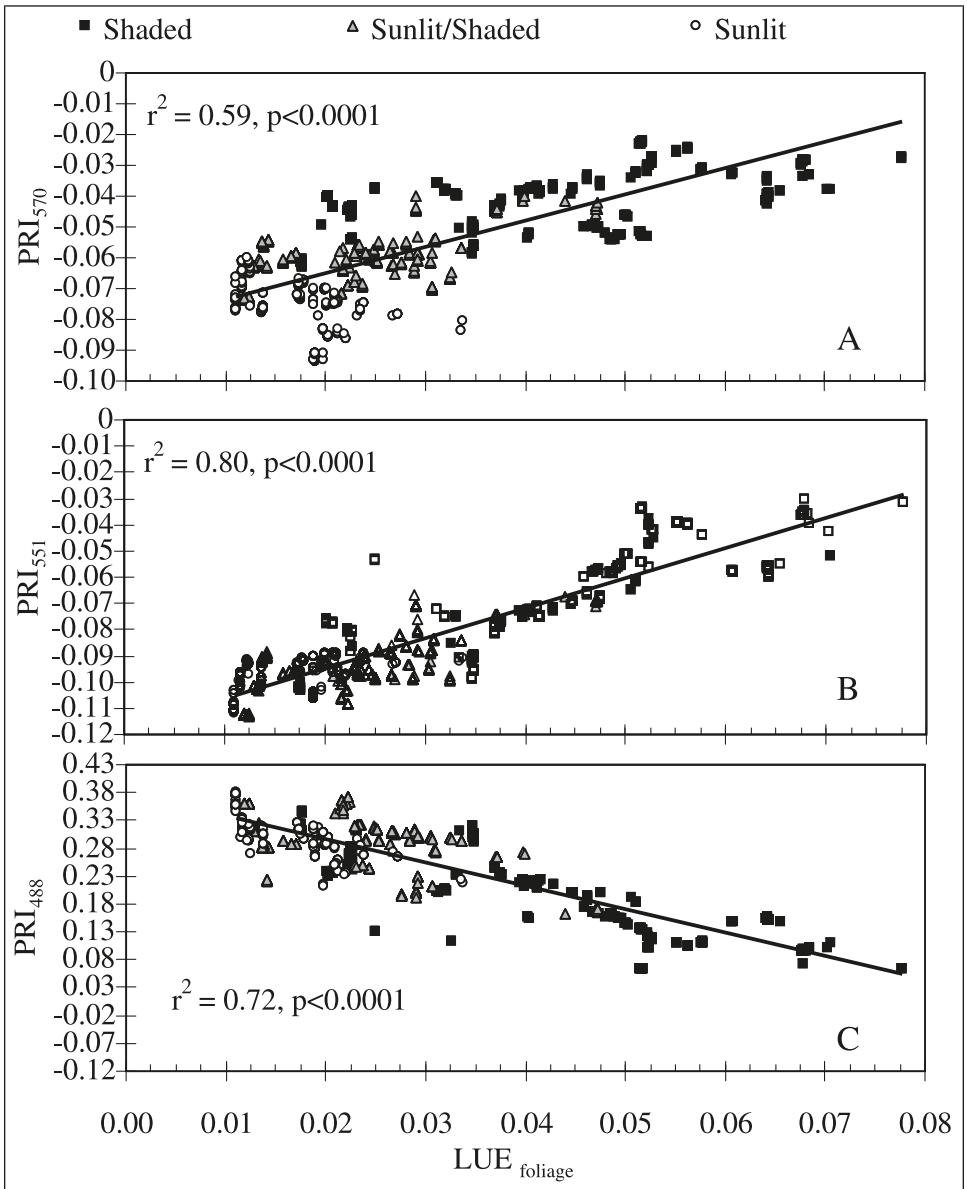

Figure 11. Linear dependence of three PRI indices on $LUE_{foliage}$ (µmol C µmol^{-1} APAR) for the three foliage groups on sunny days (n = 822): (A) PRI_{570} versus $LUE_{foliage}$ (r^2 = 0.59, P < 0.0001), where PRI_{570} (3 nm) = –0.082 + 0.8499$LUE_{foliage}$; (B) PRI_{551} versus $LUE_{foliage}$ (r^2 = 0.80, P < 0.0001), where PRI_{551} (3 nm) = –0.1177 + 1.1457$LUE_{foliage}$ and PRI_{551} (10 nm) = –0.1186 + 1.1546$LUE_{foliage}$; (C) PRI_{488} versus $LUE_{foliage}$ (r^2 = 0.72, P < 0.0001), where PRI_{488} (3 nm) = 0.379 + 4.1846$LUE_{foliage}$.

solstice, are further evidence that light levels strongly influence the responses observed.

As shown in **Figure 14**, the average midday $LUE_{foliage}$ for all foliage groups (**Figure 15A**) was lower than that for daily values (**Figure 15B**), and sunlit and mixed (shaded–sunlit) sectors had similar values in many months. In general, the average midday $LUE_{foliage}$ increased throughout the season from springtime through autumn, with some summertime depressions. This was especially evident in the shaded sectors and probably was influenced by declining incident PAR levels after the summer solstice and cooler fall temperatures, and perhaps more numerous cloudy days. It is clear from these plots that midday observations alone may not be generally representative of daily values or their seasonal trends at this site; the best correspondence between midday and daily values was obtained with the mixed foliage group. We did not include November data in these plots because of the small sample available for sunny days.

In addition to having similar daily and midday seasonal patterns, the mixed sunlit–shaded foliage group also had the closest average correspondence to the MODIS LUT value for maximum ecosystem LUE (ε_{max}) of evergreen needle forests

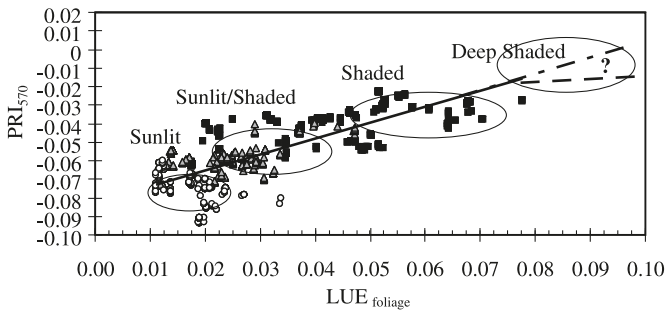

Figure 12. Conceptualization of the distribution of PRI and $LUE_{foliage}$ values for foliage exposed to a range of illumination conditions. The highest PRI and $LUE_{foliage}$ values are expected for foliage residing in the deeply shaded canopy sectors but could not be measured with the experimental setup employed in this study. Does the relationship for deeply shaded foliage receiving very low PAR (>100 $\mu mol \cdot m^{-2} \cdot s^{-1}$) continue to exhibit a linear relationship or does it plateau? Symbols as in **Figure 4**.

(0.0196 μmol C μmol^{-1} APAR; Heinsch et al., 2003). The daily $LUE_{foliage}$ values in the sunlit canopy were substantially lower than this during summer months, whereas values in the shaded foliage were typically two to three times higher. Midday $LUE_{foliage}$ values for the sunlit and mixed foliage groups were well below the MODIS LUT value in most months, but shaded foliage values were similar to the MODIS LUT value in the first half of the growing season.

Discussion

The AMPEC spectra and associated fluxes at the DF49 tower, in conjunction with ecosystem structure information, enabled the separation of the canopy foliage into three dynamic illumination categories (sunlit, shaded, and mixed shaded–sunlit) having distinct functional responses. This novel approach provided considerable insight into the diurnal and seasonal LUE heterogeneity within this forest. The dynamic behavior of LUE at the foliage level demonstrates limitations of the LUT approach using fixed LUE values.

PRI responses and photoprotection

We found that PRI values varied in complex ways for the three foliage groups, diurnally and over the season. We established that the shaded Douglas-fir canopy maintained high average PRI_{570} values (≥ –0.06) on sunny days from spring through autumn (**Figures 3A**, **4A**, **4C**), especially during mornings, and even higher average PRI_{570} values (–0.032) on cloudy days (**Figures 4B**, **4D**), conditions indicative of relatively lower light stress. Although drops in PRI values were observed at midday among all three foliage groups, the sunlit sector was most susceptible to midday PRI reductions (e.g., **Figures 3**, **5**) associated with potentially excessive high light conditions. The bowl-shaped diurnal PRI responses, which were most pronounced for the sunlit foliage sector (**Figure 5**) on sunny days, are consistent with light-induced accumulation

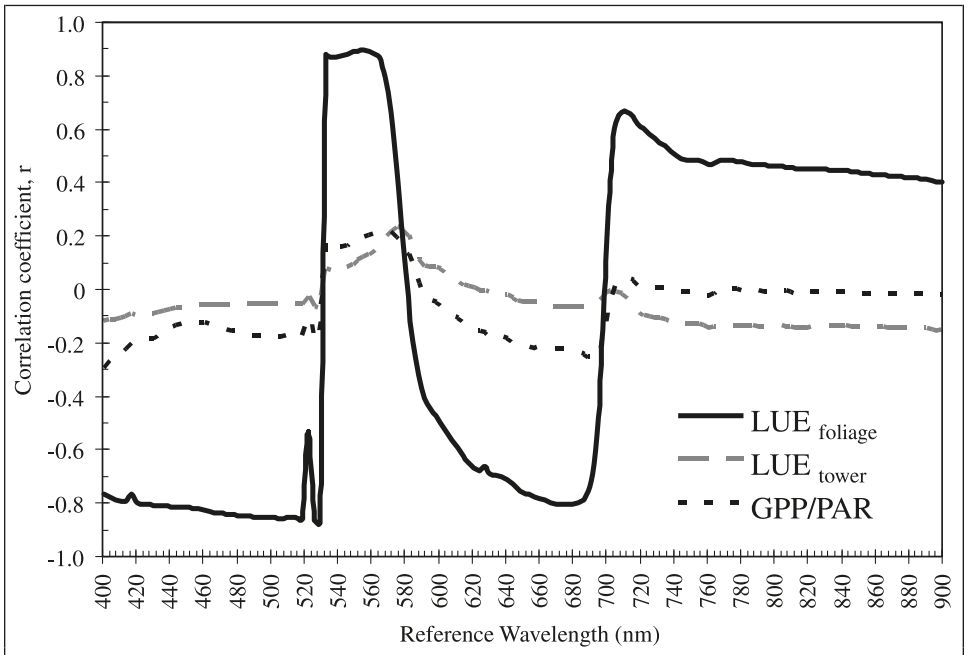

Figure 13. For all sunny day data across the 2006 season (n = 822), the correlation coefficient (r) is shown for all possible PRI indices versus LUE computed three ways: $LUE_{foliage}$, LUE_{tower}, and LUE_{canopy} (GPP/PAR). The PRI was computed with 531 nm fixed as the active band but with variable reference bands (400–900 nm). Correlations were highest for $LUE_{foliage}$ to PRI with reference wavelengths in the green (550–570 nm, $r \approx +0.90$), far-blue (~480–515 nm, $r \approx -0.85$), red (670–680, $r \approx -0.80$), and far-red regions (~710 nm, r ≈ +0.65). The two bulk canopy estimates of LUE were not highly correlated with PRI ($-0.3 > r > 0.2$).

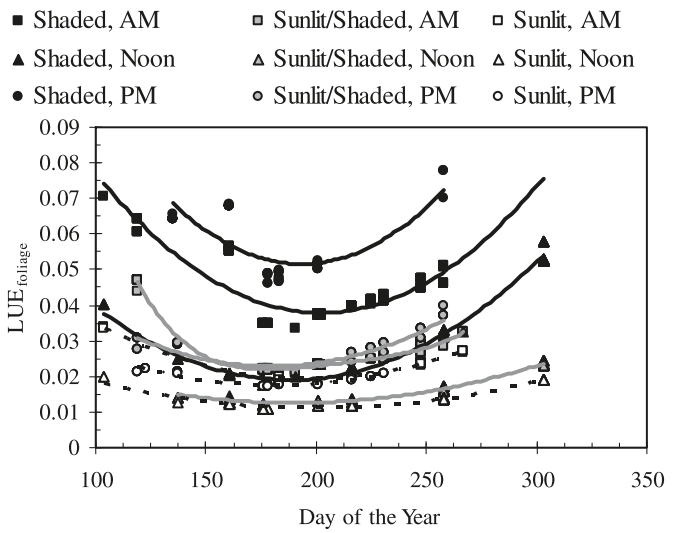

Figure 14. Seasonal courses of $LUE_{foliage}$ for the three foliage groups at three times of day for the 2006 growing season (April–November) at DF49.

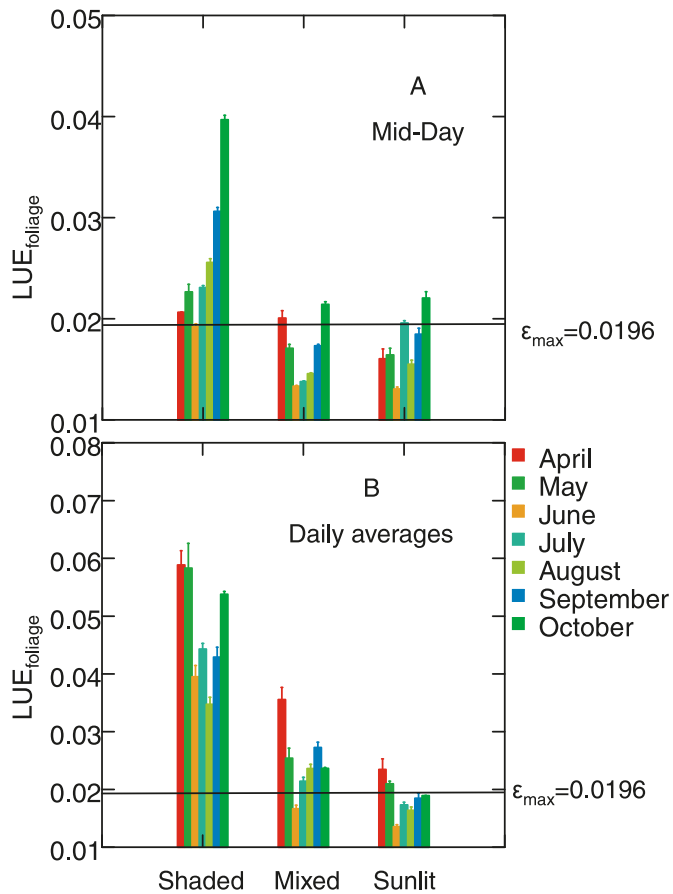

Figure 15. $LUE_{foliage}$ (µmol C µmol^{-1} APAR) by month (mean ± SE, April–November 2006) at DF49 for sunny days in the shaded (left cluster), mixed (center cluster), and sunlit (right cluster) canopy sectors: (A) at midday (10:00–2:00 pm PST; (B) daily averaged value for the same days. The MODIS LUT value for maximum ecosystem LUE (ε_{max}) of evergreen needle forests (0.0196 µmol C µmol^{-1} APAR; Heinsch et al., 2003) is shown as a horizontal line in each panel.

of zeaxanthin (Z) in foliage. On a typical sunny day, the relative concentration of Z (e.g., Z/VAZ) in healthy foliage would be expected to increase throughout the morning and decline throughout the afternoon (**Figure 5A**) as the xanthophyll pigment ratios adjust in concert with illumination conditions and are manifested as concomitant changes in PRI. This effect was probably strongly expressed in the April dataset, which captured the full diurnal expression of photosynthetic down-regulation as the forest emerged from winter into springtime with a canopy having only mature needles, and exposed to increasingly higher midday light intensities along with more favorable air temperature and soil moisture conditions (Humphreys et al., 2006). Since bud break typically occurs in May at this site (T.A. Black, personal communication), the April dataset was acquired before emergence of new (first-year) foliage.

This daily cycle represents an important short-term biochemical mechanism that adjusts the composition and function of the photosynthetic apparatus to a given light environment. However, it cannot be assumed that this process proceeds in a fixed fashion throughout the growing season. For example, branch tips in May–June displayed immature (juvenile) foliage that lacked fully developed tissues and pigment levels and might be especially vulnerable to high midday illumination at that time of year. Consequently, the $LUE_{foliage}$ values observed for the sunlit and mixed canopy sectors were lowest in May and June whether examined at midday or averaged over a day (**Figure 15**). Another example is the difference observed for April versus August midday and diurnal responses (**Figures 4**, **15**) where midday down-regulation was less in August. We speculate that one reason might be insufficient tissue water, since soil moisture was lowest in August (Humphreys et al., 2006; Cheng et al., 2009), limiting full implementation of the xanthophyll cycle because of the pH-mediated changes that underlie it. Under conditions where foliage experiences *multiple* environmental stresses under high light intensities, it may fail to exhibit strong diurnal PRI response variations.

Most important for our purposes, the MODIS LUT value for maximum ecosystem LUE (ε_{max}) of evergreen needle forests (0.0196 µmol C µmol^{-1} APAR; Heinsch et al., 2003), shown as a horizontal line in each panel, overestimated the within-canopy LUE values for sunlit and mixed foliage in most months at midday and for daily integrals (**Figure 15**). This probably means that GPP will be overestimated when derived using the MODIS fixed LUE approach, unless the required environmental variables are available and accurately describe photosynthetic down-regulation for the particular ecosystem examined, a tall order.

Acclimation responses may also explain the flatter PRI diurnal courses observed in August, since the daily xanthophyll cycle is altered when high illumination levels are sustained over time in fully developed leaves, inducing long-term light

acclimation responses that involve various biochemical, morphological, and physiological leaf-level changes (Walters, 2005). Recent studies show that repeated exposure to high light intensities caused an increase in maximum midday values for the Z/VAZ xanthophyll ratio of Norway spruce (*Picea abies* (L.) Karst.) (Štroch et al., 2008). We may have observed this phenomenon manifested as higher, constant PRI values for sunlit foliage during the August drought periods (**Figure 5B**). Of course, phenological changes were probably also occurring in late summer that affected photosynthetic function. Without understanding that light acclimation and phenology were operating in conjunction with xanthophyll cycle operation, we might wrongly misinterpret the higher August versus April PRI values from the sunlit fraction (**Figure 5B** versus **Figure 5A**) as due to lower light stress rather than the cumulative effect of various long-term leaf-level adjustments to augment photoprotection.

In addition to photoprotection responses apparently captured with PRIs due to activity of the xanthophyll cycle (e.g., PRI_{570}, **Figure 6**), chlorophyll fluorescence activity may also have been captured by EVI during the mornings (**Figure 9C**). This emerged because the EVI amplifies the red reflectance associated with the red chlorophyll fluorescence peak (as compared with NDVI). Several investigators (Van Gaalen et al., 2007; Rascher et al., 2007; Nichol et al., 2006) have recently reported that the PRI can serve as an indicator of nonphotochemical quenching, a type of photoprotection linked to chlorophyll fluorescence. Therefore, the photoprotection conveyed by the pigment system of xanthophylls is intertwined with that of chlorophylls (Meroni et al., 2008a).

Establishing the relationship of PRI to $LUE_{foliage}$

The dependence of the PRIs on solar illumination intensity was clearly revealed when the daily bowl-shaped curves (PRI versus time of day, **Figure 5**) were transformed into linear relationships for PRI versus SZA (**Figures 6**, **7**). A similar result was obtained for PRI versus PAR intensity (not shown). However, the use of above-canopy illumination conditions (e.g., SZA) yielded separate linear curves per foliage group (**Figures 6**, **7**). We demonstrated here that PRI from different foliage illumination sectors of a coniferous forest can be confounded when represented by a single, integrated, bulk canopy LUE value. Consequently, the relationship of PRI_{570} to bulk canopy LUE for this site included a large amount of scatter and was curvilinear, saturating at intermediate bulk canopy LUE values, as described in a related study elsewhere (Hilker et al., 2008a; 2008c). However, a general linear relationship for PRI versus LUE was obtained that incorporated data acquired throughout the entire growing season for all three foliage groups, when the incident within-canopy PAR illumination per group was utilized to determine $LUE_{foliage}$ (**Figures 11**, **12**).

The successful retrieval of these linear PRI–$LUE_{foliage}$ relationships relied on proper consideration of instantaneous APAR within the canopy, especially for the shaded foliage. This transformation shows that a similar physiological response was operating over all foliage groups on sunny days throughout the 2006 season and apparently accounts for short-term daily xanthophyll pigment ratio (Z/VAZ) adjustments to light intensities and the suite of leaf-level responses involved in long-term light acclimation under sustained clear-sky conditions. For example, drought or nutrient conditions that cause a more acidic lumen pH could contribute to or amplify the light-induced lumen pH reductions that initiate the xanthophyll de-epoxidation cycle (e.g., Pfundel and Dilley, 1993). However, the ability to derive linear relationships between the PRI indices and $LUE_{foliage}$ validates the hypothesis that the intensity of the light environment is primarily responsible for the PRI responses, as does the repeated recoveries from high light-induced down-regulation throughout the season, as indicated by higher PRI values on cloudy days (**Figure 4B**).

We observed seasonal changes in $LUE_{foliage}$ for all three foliage groups (**Figures 14**, **15**) related to the combined effects of phenology, acclimation, drought, etc. Our seasonal courses for $LUE_{foliage}$ highlight a possible source of error in the use of a fixed ecosystem LUE value, as in the MODIS LUT, for studies of carbon uptake dynamics. Our findings for this Douglas-fir forest are consistent with results recently published for instrumented tower sites in Saskatchewan, Canada (Drolet et al., 2008a), which also found that midday LUE_{canopy} determined from tower fluxes often fell far below the MODIS LUT values for LUE of sites across three broadly defined biomes (evergreen needle leaf forest, mixed forest, and open shrub land).

Within each foliage group, the average daily $LUE_{foliage}$ values per month exhibit the same bowl-shaped responses over time as those shown earlier for diurnal PRI responses (**Figure 5**) but are centered on June instead of solar noon, again demonstrating the importance of radiation intensity levels and associated environmental factors such as air and soil temperature. Similarly, a midsummer depression in daily LUE_{canopy} has been observed at flux towers in other ecosystems (e.g., Drolet et al., 2008b); we discovered that this occurred in all foliage sectors. However, the mixed (shaded–sunlit) group should be representative of the largest canopy foliage fraction at any time and, therefore, the most useful in estimating full LUE_{canopy}.

Implications for remote sensing

This study shows the important benefit to be gained from high-resolution information when hyperspectral reflectance is collected frequently over ecologically meaningful sectors in the canopy profile. Our results provide additional evidence to support the fundamental relationship between PRI and LUE at the leaf level, as described by many previous investigators (e.g., Gamon et al., 1990; 1992; 1993; 1997; 2001), and also provide a new understanding of the PRI and LUE dynamics. We also demonstrate the variability in $LUE_{foliage}$ across the growing season and the discrepancy between our dynamic estimates and the fixed biome-level LUT value used in carbon models for this

forest type. Our results also highlight the importance of considering canopy-structure-related information, such as light transmission and leaf distribution profiles, in utilizing spectral information to monitor canopy physiology. If it is important to know the relative contributions from the three functional canopy sectors, a weighting factor for the fractional daily representation (f) of each group could be used to estimate LUE_{canopy}, as the sum of $LUE_{foliage}(n)f(n)$. Obtaining estimates of f would require some complementary remote sensing observations acquired above the canopy with broadband optical data or laser measurements made from either above or below the canopy.

This study demonstrates that physiological dynamics, specifically for carbon uptake efficiency, can be monitored with one of several remote spectral PRI indices as long as the within-canopy incident light environment (as compared to the above-canopy incident light environment) is utilized to derive LUE for foliage within illumination sectors ($LUE_{foliage}$). However, daily $LUE_{foliage}$ exhibited a different seasonal pattern than midday $LUE_{foliage}$, which could influence interpretations of PRI acquired from midday satellite sensors. In contrast with the PRIs, the NDVI exhibited little variation with illumination conditions and no differences associated with the foliage sets, indicating that physiological responses were not the dominant factors underlying the response for this index but reaffirming its use for f_{APAR} in our calculations of dynamic $LUE_{foliage}$ in the three foliage sectors (sunlit, shaded, shaded–sunlit) throughout the growing season.

High correlations were expected among the three PRI indices; however, the superior performance of the PRI_{551} over the PRI_{570} in relation to $LUE_{foliage}$ emerged because we focused on sunny days when the xanthophyll photoprotection cycle was likely to be activated. However, the greater success for PRI_{551} was somewhat unexpected because Hall et al. (2008) found that reflectance changes near 570 nm had a slightly higher correlation with LUE for a related but more limited analysis at this site. That finding was based on bulk canopy LUE (instead of $LUE_{foliage}$), however, a BRDF-normalization to a standard high sun condition (noon on the summer solstice), and included data from a wide range of sky conditions (instead of sunny days only). Indeed, in a subsequent study undertaken by us to further exploit the full seasonal potential of this dataset, we have recently found that both PRI_{570} and PRI_{551} exhibited higher and more seasonally stable correlations with LUE examined over the whole growing season as compared with many other spectral indices (Cheng et al., 2009). Consequently, we believe that any narrow (3–10 nm) green reference band within the 545–575 nm waveband would be suitable to obtain PRI as long as the physiologically critical waveband at 531 nm is utilized. However, the finding that comparable (or better) results can be obtained with PRI_{551} across canopy sectors throughout a growing season (r^2 = 0.80) gives us confidence that physiologically useful retrievals of bulk canopy LUE can be achieved from satellite data using the corresponding MODIS PRI_{551} based on 10 nm wide "ocean" bands (Middleton et al., 2004; Drolet et al., 2005; 2008a).

Our results provide a framework to develop two separate avenues of investigation: (*i*) insight into interpreting spectral LUE retrievals from space, and (*ii*) understanding high light-induced physiological stress leading to reductions in photosynthetic efficiency (e.g., nonphotochemical quenching) at the canopy level.

Summary

We have provided clear evidence that light-use efficiency (LUE) can be well described within a coniferous forest when the foliage is partitioned into three groups according to their illumination conditions (sunlit, shaded, and mixed shaded–sunlit), that a single linear relationship relating photochemical reflectance indices (PRIs; especially for PRI_{551}) across all three foliage groups to $LUE_{foliage}$ exists on relatively clear sky days, and that $LUE_{foliage}$ was highly variable across the 2006 growing season at Canadian Douglas-fir forest DF49. The seasonal patterns for monthly $LUE_{foliage}$ estimates were different for midday versus daily values, with significantly lower estimates obtained from midday observations (0.015–0.038 μmol C μmol^{-1} APAR) as compared with daily values (0.02–0.06 μmol C μmol^{-1} APAR). We affirmed the four hypotheses set forth at the outset. This study supports the use of PRI for remotely estimating LUE, given the in situ light environment per foliage group, and provides a physiological basis for interpretation of remotely acquired PRI for a coniferous forest.

Acknowledgments

This research was supported by National Aeronautics and Space Administration (NASA) Research Opportunities in Space and Earth Sciences (ROSES) funding through the Carbon Cycle Science Program (Diane Wickland, Manager). Yen-Ben Cheng was supported through the NASA Postdoctoral Program, administered by Oak Ridge Associated Universities. Thomas Hilker was partially funded by a postgraduate scholarship of the German Academic Exchange Service (DAAD), a Natural Sciences and Engineering Research Council of Canada (NSERC) Discovery Grant to Nicholas Coops, and funds provided to the University of British Columbia (UBC) from the Comprehensive Community Plan (CCP), NSERC, and BIOCAP. We acknowledge the following people for their assistance in technical design, installation, and maintenance of the radiometer platform: Zoran Nesic, Dominic Lessard, Rick Ketler, and Andrew Sauter from UBC Faculty of Land and Food Systems (LFS).

References

Adams, W.W., and Demmig-Adams, B. 1994. Carotenoid composition and down regulation of photosystem II in three conifer species during the winter. *Physiologia Plantarum*, Vol. 92, pp. 451–458.

Adams, W.W., Demmig-Adams, B., Logan, B.A., Barker, D.H., and Osmond, C.B. 1999. Rapid changes in xanthophyll cycle-dependent energy

dissipation and photosystem II efficiency in two vines, *Stephania Japonica* and *Smilax Australis*, growing in the understory of an open Eucalyptus forest. *Plant Cell and Environment*, Vol. 22, pp. 125–136.

Adams, W.W., Demmig-Adams, B., Rosenstiel, T.N., Brightwell, A.K., and Ebbert, V. 2002. Photosynthesis and photoprotection in overwintering plants. *Plant Biology*, Vol. 4, pp. 545–557.

Ahl, D.E., Gower, S.T., Mackay, D.S., Burrows, S.N., Norman, J.M., and Diak, G. 2004. Light use efficiency of a heterogeneous forest in northern Wisconsin: implications for remote sensing and modeling net primary production. *Remote Sensing of Environment*, Vol. 93, pp. 168–178.

Alton, P.B., North, P.R., and Los, S.O. 2007. The impact of diffuse sunlight on canopy light-use efficiency, gross photosynthetic product and net ecosystem exchange in three forest biomes. *Global Change Biology*, Vol. 13, pp. 776–787.

Baldocchi, D.D. 2003. Assessing the eddy covariance technique for evaluating carbon dioxide exchange rates of ecosystems: past, present and future. *Global Change Biology*, Vol. 9, pp. 479–492.

Baldocchi, D., Falge, E., Gu, L.H., Olson, R., Hollinger, D., Running, S., Anthoni, P., Bernhofer, C., Davis, K., Evans, R., Fuentes, J., Goldstein, A., Katul, G., Law, B., Lee, X.H., Malhi, Y., Meyers, T., Munger, W., Oechel, W., Paw, U.K.T., Pilegaard, K., Schmid, H.P., Valentini, R., Verma, S., Vesala, T., Wilson, K., and Wofsy, S. 2001. Fluxnet: A new tool to study the temporal and spatial variability of ecosystem-scale carbon dioxide, water vapor, and energy flux densities. *Bulletin of the American Meteorological Society*, Vol. 82, pp. 2415–2434.

Barton, C.V.M., and North, P.R.J. 2001. Remote sensing of canopy light use efficiency using the photochemical reflectance index: model and sensitivity analysis. *Remote Sensing of Environment*, Vol. 78, pp. 264–273.

Bilger, W., and Björkman, O. 1990. Role of the xanthophyll cycle in photoprotection elucidated by measurements of light-induced absorbance changes, fluorescence and photosynthesis in leaves of *Hedera canariensis*. *Photosynthesis Research*, Vol. 25, pp. 173–185.

Bilger, W., Björkman, O., and Thayer, S. 1989. Light-induced spectral absorbance changes in relation to photosynthesis and the epoxidation state of xanthophyll cycle components in cotton leaves. *Plant Physiology*, Vol. 91, pp. 542–551.

Black, T.A., Denhartog, G., Neumann, H.H., Blanken, P.D., Yang, P.C., Russell, C., Nesic, Z., Lee, X., Chen, S.G., Staebler, R., and Novak, M.D. 1996. Annual cycles of water vapour and carbon dioxide fluxes in and above a boreal aspen forest. *Global Change Biology*, Vol. 2, pp. 219–229.

Boardman, N. 1977. Comparative photosynthesis of sun and shade plants. *Annual Review of Plant Physiology*, Vol. 28, pp. 355–377.

Brodersen, C.R., Vogelmann, T.C., Williams, W.E., and Gorton, H.L. 2008. A new paradigm in leaf-level photosynthesis: direct and diffuse lights are not equal. *Plant, Cell and Environment*, Vol. 31, pp. 159–164.

Cai, T., Flanagan, L.G., Jassel, R.S., and Black, R.A. 2008. Modelling environmental controls on ecosystem photosynthesis and the carbon isotope composition of ecosystem-respired CO_2 in a coastal Douglas-fir forest. *Plant, Cell and Environment*, Vol. 31, pp. 435–453.

Chen, J.M. 1996. Canopy architecture and remote sensing of the fraction of photosynthetically active radiation absorbed by boreal conifer forests. *IEEE Transactions on Geoscience and Remote Sensing*, Vol. 34, pp. 1353–1368.

Chen, J.M., and Black, T.A. 1991. Measuring leaf-area index of plant canopies with branch architecture. *Agricultural and Forest Meteorology*, Vol. 57, pp. 1–12.

Chen, J.M., Govind, A., Sonnentag, O., Zhang, Y., Barr, A., and Amiro, B. 2006. Leaf area index measurements at Fluxnet Canada forest sites. *Agricultural and Forest Meteorology*, Vol. 140, pp. 257–268.

Cheng, Y.-B., Middleton, E.M., Hilker, T., Coops, N.C., Black, T.A., and Krishnan, P. 2009. Dynamics of spectral bio-indicators and their correlations with light use efficiency using directional observations at a Douglas-fir forest. *Measurement Science and Technology*. In press.

Coops, N.C., Hilker, T., Wulder, M.A., St-Onge, B., Newnham, G., Siggins, A., and Trofymow, J.A. 2007a. Estimating canopy structure of Douglas-fir forest stands from discrete-return lidar. *Trees-Structure and Function*, Vol. 21, pp. 295–310.

Coops, N.C., Black, T.A., Jassal, R.S., Trofymow, J.A., and Morgenstern, K. 2007b. Comparison of MODIS, eddy covariance determined and physiologically modelled gross primary production (GPP) in a Douglas-fir forest stand. *Remote Sensing of Environment*, Vol. 107, pp. 385–401.

Demmig-Adams, B. 1990. Carotenoids and photoprotection in plants — a role for the xanthophyll zeaxanthin. *Biochemica et Biophysica Acta*, Vol. 1020, pp. 1–24.

Demmig-Adams, B. 1998. Survey of thermal energy dissipation and pigment composition in sun and shade leaves. *Plant and Cell Physiology*, Vol. 39, pp. 474–482.

Demmig-Adams, B., and Adams, W.W., III. 1992. Photoprotection and other responses of plants to light stress. *Annual Review of Plant Physiology and Molecular Biology*, Vol. 43, pp. 599–626.

Demmig-Adams, B., and Adams, W.W., III. 1996. The role of the xanthophylls cycle carotenoids in the protection of photosynthesis. *Trends in Plant Science*, Vol. 1, pp. 21–26.

Demmig-Adams, B., and Adams, W.W., III. 2006. Photoprotection in an ecological context: the remarkable complexity of thermal energy dissipation. *New Phytologist*, Vol. 172, pp. 11–21.

Demmig-Adams, B., Gilmore, A.M., and Adams, W.W., III. 1996. Carotenoids 3: in vivo functions of carotenoids in higher plants. *FASEB Journal*, Vol. 10, pp. 403–412.

Demmig-Adams, B., Moeller, D.L., Logan, B.A., and Adams, W.W., III. 1998. Positive correlation between levels of retained zeaxanthin plus antheraxanthin and degree of photoinhibition in shade leaves of *Schefflera arboricola* (Hayata) Merrill. *Planta*, Vol. 205, pp. 367–374.

Drewitt, G.B., Black, T.A., Nesic, Z., Humphreys, E.R., Jork, E.M., Swanson, R., Ethier, G.J., Griffis, T., and Morgenstern, K. 2002. Measuring forest floor CO_2 fluxes in a Douglas-fir forest. *Agriculture and Forest Meteorology*, Vol. 110, pp. 299–317.

Drolet, G.G., Huemmrich, K.F., Hall, F.G., Middleton, E.M., Black, T.A., Barr, A.G., and Margolis, H.A. 2005. A MODIS-derived photochemical reflectance index to detect inter-annual variations in the photosynthetic light-use efficiency of a boreal deciduous forest. *Remote Sensing of Environment*, Vol. 98, pp. 212–224.

Drolet, G.G., Middleton, E.M., Huemmrich, K.F., Hall, F.G., Margolis, H.A., Amiro, R., Barr, A., and Black, A. 2008a. Regional mapping of gross light-use efficiency using MODIS spectral indices. *Remote Sensing of Environment*, Vol. 12, No. 6, pp. 3064–3078.

Drolet, G., Margolis, H., Piao, S., and Middleton, E.M. 2008b. Midsummer and autumn depressions in net carbon fluxes and light-use efficiency across the circumpolar boreal forest. In *Proceedings of the European Geosciences Union General Assembly*, 13–18 April 2008, Vienna, Austria. European Geosciences Union, Katlenburg-Lindau, Germany.

Evain, S., Flexas, J., and Moya, I. 2004. A new instrument for passive remote sensing: 2. Measurement of leaf and canopy reflectance changes at 531 nm and their relationship with photosynthesis and chlorophyll fluorescence. *Remote Sensing of Environment*, Vol. 91, pp. 175–185.

Filella, I., Amaro, T., Araus, J.L., and Peñuelas, J. 1996. Relationship between photosynthetic radiation-use efficiency of barley canopies and the photochemical reflectance index (PRI). *Physiologia Plantarum*, Vol. 96, pp. 211–216.

Gamon, J.A., Field, C.B., Bilger, W., Björkman, O., Fredeen, A.L., and Peñuelas, J. 1990. Remote sensing of the xanthophyll cycle and chlorophyll fluorescence in sunflower leaves and canopies. *Oecologia*, Vol. 85, pp. 1–7.

Gamon, J.A., Penuelas, J., and Field, C.B. 1992. A narrow-waveband spectral index that tracks diurnal changes in photosynthetic efficiency. *Remote Sensing of Environment*, Vol. 41, pp. 35–44.

Gamon, J.A., Filella, I., and Penuelas, J. 1993. The dynamic 531-nanometer Δ reflectance signal: a survey of twenty angiosperm species. In *Photosynthetic responses to the environment*. Edited by H.Y. Yamamoto and C.M. Smith. American Society of Plant Physiologists, Rockville, Md. pp. 172–177.

Gamon, J.A., Serrano, L., and Surfus, J.S. 1997. The photochemical reflectance index: an optical indicator of photosynthetic radiation use efficiency across species, functional types, and nutrient levels. *Oecologia*, Vol. 112, pp. 492–501.

Gamon, J.A., Field, C.B., Fredeen, A.L., and Thayer, S. 2001. Assessing photosynthetic downregulation in sunflower stands with an optically-based mode. *Photosynthesis Research*, Vol. 67, pp. 113–125.

Gilmore, A.M., and Yamasaki, H. 1998. 9-Aminoacridine and dibucaine exhibit competitive interactions and complicated inhibitory effects that interfere with measurements of ΔpH and xanthophyll cycle-dependent Photosystem II energy dissipation. *Photosynthesis Research*, Vol. 57, pp. 159–174.

Goodwin, G. 1937. *Regeneration study on the logged-off lands of the Comox Logging and Railway Company Oyster River.* Forest Survey R72 (survey file No. 0124780). British Columbia Forest Service, Victoria, B.C. 39 pp. and map.

Goulden, M.L., Daube, B.C., Fan, S.-M., Sutton, D.J., Bazzaz, A., Munger, J.W., and Wofsy, S.C. 1997. Physiological responses of a black spruce forest to weather. *Journal of Geophysical Research*, Vol. 102, No. D4, pp. 28 987 – 28 996.

Goward, S.N., and Huemmrich, K.F. 1992. Vegetation canopy PAR absorptance and the normalized difference vegetation index: an assessment using the SAIL model. *Remote Sensing of Environment*, Vol. 39, pp. 119–140.

Grace, J., Nichol, C.J., Disney, M., Lewis, P., and Quaife, T. 2007. Can we measure terrestrial photosynthetic rate from space? *Global Change Biology*, Vol. 13, pp. 1–14.

Guo, J.M., and Trotter, C.M. 2004. Estimating photosynthetic light-use efficiency using the photochemical reflectance index: variations among species. *Functional Plant Biology*, Vol. 31, pp. 255–265.

Hall, F.G., Hilker, T., Coops, N.C., Lyapustin, A., Huemmrich, K.F., Middleton, E.M., Margolis, H.A., and Drolet, G.G. 2008. Multi-angle remote sensing of forest light use efficiency by observing PRI variation with canopy shadow fraction. *Remote Sensing of Environment*, Vol. 112, No. 7, pp. 3201–3211.

Havaux, M., and Niyogi, K.K. 1999. The violaxanthin cycle protects plants from photooxidative damage by more than one mechanism. *Proceedings of the National Academy of Sciences of the USA*, Vol. 96, pp. 8762–8767.

Heinsch, F.A., Reeves, M., Votava, P., Kang, S., Milesi, C., Zhao, M., Glassy, J., Jolly, W.M., Loehman, R., Bowker, D.F., Kimball, J.S., Nemani, R.R., and Running, S.W. 2003. *User's guide: GPP and NPP (MOD17A2/A3) products: NASA MODIS land algorithm, version 1.3*. University of Montana, Missoula, Mont. Available from www.ntsg.umt.edu/modis/MOD17UsersGuide.pdf.

Heinsch, F.A., Zhao, M., Running, S.W., Kimball, J.S., Nemani, R.R., Davis, K.J., Bolstad, P.V., Cook, B.D., Desai, A.R., Ricciuto, D.M., Law, B.E., Oechel, W.C., Kwon, H.J., Luo, H., Wofsy, S.C., Dunn, A.L., Munger, J.W., Baldocchi, D.D., Xu, L., Hollinger, D.Y., Richardson, A.D., Stoy, P.C., Siqueira, M.B.S., Monson, R.K., Burns, S.P., and Flanagan, L.B. 2006. Evaluation of remote sensing based terrestrial productivity from MODIS using regional tower eddy flux network observations. *IEEE Transactions on Geoscience and Remote Sensing*, Vol. 44, pp. 1908–1925.

Hilker, T., Coops, N.C., Nesic, Z., Wulder, M.A., and Black, A.T. 2007. Instrumentation and approach for unattended year round tower based measurements of spectral reflectance. *Computers and Electronics in Agriculture*, Vol. 56, pp. 72–84.

Hilker, T., Coops, N.C., Hall, F.G., Black, T.A., Wulder, M.A., Nesic, Z., and Krishnan, P. 2008a. Separating physiologically and directionally induced changes in PRI using BRDF models. *Remote Sensing of Environment*, Vol. 112, pp. 2777–2788.

Hilker, T., Coops, N.C., Schwalm, C.R., Jassal, R.S., Black, T.A., and Krishnan, P. 2008b. Effects of mutual shading of tree crowns on prediction of photosynthetic light use efficiency in a coastal Douglas-fir forest. *Tree Physiology*, Vol. 28, pp. 825–834.

Hilker, T., Coops, N.C., Hall, F.G., Black, T.A., Chen, B., Krishnan, P., Wulder, M.A., Sellers, P.J., Middleton, E.M., and Huemmrich, K.F. 2008c. A modeling approach for upscaling gross ecosystem production to the landscape scale using remote sensing data. *Journal of Geophysical Research — Biogeosciences*, Vol. 113, G03006. doi:10.1029/2007JG000666.

Huemmrich, K.F., Privette, J.L., Mukufute, M., Myneni, R.B., and Knyazikhin, Y. 2005. Time-series validation of MODIS land biophysical products in a Kalahari woodland. *International Journal of Remote Sensing*, Vol. 26, pp. 4381–4398.

Huete, A.R., Justice, C., and Liu, H. 1994. Development of vegetation and soil indices for MODIS-EOS. *Remote Sensing of Environment*, Vol. 49, pp. 224–234.

Huete, A.R., Didan, K., Miura, T., Rodriguez, E.P., Gao, X., and Ferreira, L.G. 2002. Overview of the radiometric and biophysical performance of the MODIS vegetation indices. *Remote Sensing of Environment*, Vol. 83, pp. 195–213.

Humphreys, E.R., Black, T.A., Morgenstern, K., Cai, T.B., Drewitt, G.B., Nesic, Z., and Trofymow, J.A. 2006. Carbon dioxide fluxes in coastal Douglas-fir stands at different stages of development after clearcut harvesting. *Agricultural and Forest Meteorology*, Vol. 140, pp. 6–22.

Inoue, Y., and Peñuelas, J. 2006. Relationship between light use efficiency and photochemical reflectance index in soybean leaves as affected by soil water content. *International Journal of Remote Sensing*, Vol. 27, pp. 5109–5114.

Inoue, Y., Peñuelas, J., Miyata, A., and Mano, M. 2008. Normalized difference spectral indices for estimating photosynthetic efficiency and capacity at a canopy scale derived from hyperspectral and CO_2 flux measurements in rice. *Remote Sensing of Environment*, Vol. 112, pp. 156–172.

Jassal, R.S., Black, T.A., Cai, T.B., Morgenstern, K., Li, Z., Gaumont-Guay, D., and Nesic, Z. 2007. Components of ecosystem respiration and an estimate of net primary productivity of an intermediate-aged Douglas-fir stand. *Agricultural and Forest Meteorology*, Vol. 144, pp. 44–57.

Jenkins, J., Richardson, A.D., Braswell, B.H., Ollinger, S.V., Hollinger, D.Y., and Smith, M.L. 2007. Refining light-use efficiency calculations for a deciduous forest canopy using simultaneous tower-based carbon flux and radiometric measurements. *Agricultural and Forest Meteorology*, Vol. 143, pp. 64–79.

Jones, H.G. 1983. *Plants and microclimate, a quantitative approach to environmental plant physiology*. Cambridge University Press, Cambridge, U.K. 323 pp.

Justice, C.O., Vermote, E., Townshend, J.R.G., Defries, R., Roy, D.P., Hall, D.K., Salomonson, V.V., Privette, J.L., Riggs, G., Strahler, A., Lucht, W., Myneni, R.B., Knyazikhin, Y., Running, S.W., Nemani, R.R., Wan, Z.M., Huete, A.R., Van Leeuwen, W., Wolfe, R.E., Giglio, L., Muller, J.P., Lewis, P., and Barnsley, M.J. 1998. The moderate resolution imaging spectroradiometer (MODIS): land remote sensing for global change research. *IEEE Transactions on Geoscience and Remote Sensing*, Vol. 36, pp. 1228–1249.

Klinka, K., Pojar, J., and Meidinger, D.V. 1991. Revision of biogeoclimatic units of coastal British Columbia. *Northwest Science*, Vol. 65, pp. 32–47.

Krishnan, P., Black, T.A., Grant, N.J., Barr, A.G., Hogg, E.H., Jassal, R.S., and Morgenstern, K. 2006. Impact of changing soil moisture distribution on net ecosystem productivity of a boreal aspen forest during and following drought. *Agricultural and Forest Meteorology*, Vol. 139, pp. 208–223.

Krishnan, P., Black, T.A., Barr, A.G., Grant, N.J., Gaumont-Guay, D., and Nesic, Z. 2008. Factors controlling the interannual variability in the carbon balance of a southern boreal black spruce forest. *Journal of Geophysical Research*, Vol. 113, No. D09109. doi:10.1029/2007JD008965.

Krishnan, P., Black, T.A., Jassal, R., and Nesic, Z. 2009. Interannual variability of the carbon balance of three different-aged Douglas-fir stands in the Pacific Northwest. *Journal of Geophysical Research — Biogeosciences*. In press.

Kurasová, I., Kalina, J., Urban, O., Štroch, M., and Špunda, V. 2003. Acclimation of two distinct plant species, spring barley and Norway spruce, to combined effect of various irradiance and CO_2 concentration during cultivation in controlled environment. *Photosynthetica*, Vol. 41, No. 4, pp. 513–523.

Lagergren, F., Eklundh, L., Grelle, A., Lundblad, M., Mölder, M., Lankreijer, H., and Lindroth, A. 2005. Net primary production and light use efficiency in a mixed coniferous forest in Sweden. *Plant Cell and Environment*, Vol. 28, pp. 412–423.

Larcher, W. 1987. Stress in plants. *Naturwissenschaften*, Vol. 74, pp. 158–167.

Lichtenthaler, H.K. 1996. Vegetation stress: an introduction to the stress concept in plants. *Journal of Plant Physiology*, Vol. 148, pp. 4–14.

Lichtenthaler, H., Buschmann, C., Döll, M., Fietz, H.J., Bach, T., Kozel, U., Meier, D., and Rahmsdorf, U. 1981. Photosynthetic activity, chloroplast ultrastructure, and leaf characteristics of high-light and low-light plants and of sun and shade leaves. *Photosynthesis Research*, Vol. 2, pp. 115–141.

Lichtenthaler, H.K., Ač, A., Marek, M.V., Kalina, J., and Urban, O. 2007. Differences in pigment composition, photosynthetic rates and chlorophyll fluorescence images of sun and shade leaves of four tree species. *Plant Physiology and Biochemistry*, Vol. 45, pp. 577–588.

Louis, J., Ounis, A., Ducruet, J.M., Evain, S., Laurila, T., Thum, T., Aurela, M., Wingsle, G., Alonso, L., Pedros, R., and Moya, I. 2005. Remote sensing of sunlight-induced chlorophyll fluorescence and reflectance of Scots pine in the boreal forest during spring recovery. *Remote Sensing of Environment*, Vol. 96, pp. 37–48.

Margolis, H.A., Flanagan, L.B., and Amiro, B.D. 2006. The Fluxnet-Canada Research Network: influence of climate and disturbance on carbon cycling in forests and peatlands. *Agriculture and Forest Meteorology*, Vol. 140, pp. 1–5.

Meroni, M., Picchi, V., Rossini, M., Cogliati, S., Panigada, C., Nali, C., Lorenzini, G., and Colombo, R. 2008a. Leaf level early assessment of ozone injuries by passive fluorescence and PRI. *International Journal of Remote Sensing*, Vol. 29, No. 17–18, pp. 5409–5422.

Meroni, M., Rossini, M., Picchi, V., Panigada, C., Cogliati, S., Nali, C., and Colombo, R. 2008b. Assessing steady-state fluorescence and PRI from hyperspectral proximal sensing as early indicators of plant stress. *Sensors*, Vol. 8, pp. 1740–1754.

Middleton, E.M., Drolet, G., Huemmrich, K.F., Hall, F.G., Knox, R.G., Black, A., Barr, A., Lyapustin, A.I., Gervin, J.C., and Margolis, H. 2004. Direct satellite inference of ecosystem light use efficiency for carbon exchange using MODIS on Terra and Aqua. In *IGARSS'04, Proceedings of the International Geoscience and Remote Sensing Symposium*, 19–24 September 2004, Anchorage, Alaska. CD-ROM. IEEE, Piscataway, N.J. 4 pp.

Monteith, J.L. 1972. Solar-radiation and productivity in tropical ecosystems. *Journal of Applied Ecology*, Vol. 9, pp. 747–766.

Monteith, J.L. 1977. Climate and efficiency of crop production in Britain. *Philosophical Transactions of the Royal Society of London B: Biological Sciences*, Vol. 281, pp. 271–294.

Morgenstern, K., Black, T.A., Humphreys, E.R., Griffis, T.J., Drewitt, G.B., Cai, T.B., Nesic, Z., Spittlehouse, D.L., and Livingston, N.J. 2004. Sensitivity and uncertainty of the carbon balance of a Pacific Northwest Douglas-fir forest during an El Nino/La Nina cycle. *Agricultural and Forest Meteorology*, Vol. 123, pp. 201–219.

Müller, P., Li, X.-P., and Niyogi, K.K. 2001. Non-photochemical quenching: a response to excess light energy. *Plant Physiology*, Vol. 125, pp. 1558–1566.

Nichol, C.J., Huemmrich, K.F., Black, T.A., Jarvis, P.G., Walthall, C.L., Grace, J., and Hall, F.G. 2000. Remote sensing of photosynthetic-light-use efficiency of a boreal forest. *Agricultural and Forest Meteorology*, Vol. 101, pp. 131–142.

Nichol, C.J., Lloyd, J., Shibistova, O., Arneth, A., Roser, C., Knohl, A., Matsubara, S., and Grace, J. 2002. Remote sensing of photosynthetic-light-use efficiency of a Siberian boreal forest. *Tellus Series B — Chemical and Physical Meteorology*, Vol. 54, pp. 677–687.

Nichol, C.J., Rascher, U., Matsubara, S., and Osmond, B. 2006. Assessing photosynthetic efficiency in an experimental mangrove canopy using remote sensing and chlorophyll fluorescence. *Trees — Structure and Function*, Vol. 20, pp. 9–15.

Öquist, G., and Huner, N.P.A. 2003. Photosynthesis of overwintering evergreen plants. *Annual Review of Plant Biology*, Vol. 54, pp. 329–355.

Parker, G.G., Harmon, M.E., Lefsky, M.A., Chen, J., Van Pelt, R., Weiss, S.B., Thomas, S.C., Winner, W.E., Shaw, D.C., and Franklin, J.F. 2004. Three dimensional structure of an old-growth *Pseudotsuga–Tsuga* canopy and its implications for radiation balance, microclimate, and atmospheric gas exchange. *Ecosystems*, Vol. 7, pp. 440–453. doi:10.1007/s10021-004-0136-5.

Papale, D., Reichstein, M., Aubinet, M., Canfora, E., Bernhofer, C., Kutch, W., Longdoz, B., Rambal, S., Valentini, R., Vesala, T., and Yakir, D. 2006. Towards a standardized processing of net ecosystem exchange measured

with eddy covariance technique: algorithms and uncertainty estimation. *Biogeosciences*, Vol. 3, pp. 571–583.

Peñuelas, J., Gamon, J.A., Fredeen, A.L., Merino, J., and Field, C.B. 1994. Reflectance indices associated with physiological changes in nitrogen- and water-limited sunflower leaves. *Remote Sensing of Environment*, Vol. 48, pp. 135–146.

Peñuelas, J., Filella, I., and Gamon, J.A. 1995. Assessment of photosynthetic radiation-use efficiency with spectral reflectance. *New Phytologist*, Vol. 131, pp. 291–296.

Peñuelas, J., Llusia, J., Pinol, J., and Filella, I. 1997. Photochemical reflectance index and leaf photosynthetic radiation-use-efficiency assessment in Mediterranean trees. *International Journal of Remote Sensing*, Vol. 18, No. 13, pp. 2863–2868.

Pfundel, E., and Bilger, W. 1994. Regulation and possible function of the violaxanthin cycle. *Photosynthesis Research*, Vol. 42, pp. 89–109.

Pfundel, E.E., and Dilley, R.A. 1993. The pH dependence of violaxanthin deepoxidation in isolated pea chloroplasts. *Plant Physiology*, Vol. 101, pp. 65–71.

Potter, C.S., Randerson, J.T., Field, C.B., Matson, P.A., Vitousek, P.M., Mooney, H.A., and Klooster, S.A. 1993. Terrestrial ecosystem production — a process model based on global satellite and surface data. *Global Biogeochemical Cycles*, Vol. 7, pp. 811–841.

Rahman, A.F., Gamon, J.A., Fuentes, D.A., Roberts, D., and Prentiss, D. 2001. Modeling spatially distributed ecosystem flux of boreal forest using hyperspectral indices from AVIRIS imagery. *Journal of Geophysical Research*, Vol. 106, No. D24, pp. 33 579 – 33 591.

Rahman, A.F., Cordova, V.D., Gamon, J.A., Schmid, H.P., and Sims, D.A. 2004. Potential of MODIS ocean bands for estimating CO_2 flux from terrestrial vegetation: A novel approach. *Geophysical Research Letters*, Vol. 31, No. 10, L10503.

Rascher, U., Nichol, C., Small, C., and Hendricks, L. 2007. Monitoring the spatio-temporal dynamics of photosynthesis with a portable hyperspectral imaging system. *Photogrammetric Engineering & Remote Sensing*, Vol. 73, No. 1, pp. 45–56.

Reda, I., and Andreas, A. 2004. Solar position algorithm for solar radiation applications. *Solar Energy*, Vol. 76, pp. 577–589.

Sarijeva, G., Knapp, M., and Lichtenthaler, H.K. 2006. Differences in photosynthetic activity, chlorophyll and carotenoid levels, and in chlorophyll fluorescence parameters in green sun and shade leaves of Ginkgo and Fagus. *Journal of Plant Physiology*, Vol. 164, pp. 950–955.

Schwalm, C.R., Black, T.A., Arniro, B.D., Arain, M.A., Barr, A.G., Bourque, C.P.A., Dunn, A.L., Flanagan, L.B., Giasson, M.A., Lafleur, P.M., Margolis, H.A., Mccaughey, J.H., Orchansky, A.L., and Wofsy, S.C. 2006. Photosynthetic light use efficiency of three biomes across an east–west continental-scale transect in Canada. *Agricultural and Forest Meteorology*, Vol. 140, pp. 269–286.

Sims, D.A., and Gamon, J.A. 2002. Relationships between leaf pigment content and spectral reflectance across a wide range of species, leaf structures and developmental stages. *Remote Sensing of Environment*, Vol. 81, pp. 337–354.

Špunda, V., Čajánek, M., Kalina, J., Lachetová, I., Šprtová, M., and Marek, M.V. 1998. Mechanistic differences in utilization of absorbed excitation energy within photosynthetic apparatus of Norway spruce induced by the vertical distribution of photosynthetically active radiation through the tree crown. *Plant Science*, Vol. 133, pp. 155–165.

Štroch, J., Kuldová, K., Kalina, J., and Špunda, V. 2008. Dynamics of the xanthophyll cycle and non-radiative dissipation of absorbed light energy during exposure of Norway spruce to high irradiance. *Journal of Plant Physiology*, Vol. 165, pp. 612–622.

Suárez, L., Zarco-Tejada, P.J., Sepulcre-Cantó, G., Pérez-Priego, O., Miller, J.R., Jiménez-Muñoz, J.C., and Sobrino, J. 2008. Assessing canopy PRI for water stress detection with diurnal airborne imagery. *Remote Sensing of Environment*, Vol. 112, No. 2, pp. 560–575.

Thayer, S.S., and Björkman, O. 1990. Leaf xanthophyll content and composition in sun and shade leaves. *Photosynthesis Research*, Vol. 23, pp. 331–343.

Trotter, G.M., Whitehead, D., and Pinkney, E.J. 2002. The photochemical reflectance index as a measure of photosynthetic light use efficiency for plants with varying foliar nitrogen contents. *International Journal of Remote Sensing*, Vol. 23, pp. 1207–1212.

Tucker, C.J. 1979. Red and photographic infrared linear combinations for monitoring vegetation. *Remote Sensing of Environment*, Vol. 8, pp. 127–150.

Turner, D.P., Urbanski, S., Bremer, D., Wofsy, S.C., Meyers, T., Gower, S.T., and Gregory, M. 2003. A cross-biome comparison of daily light use efficiency for gross primary production. *Global Change Biology*, Vol. 9, pp. 383–395.

Van Den Eeckhaut, M., Poesen, J., Verstraeten, G., Vanacker, V., Moeyersons, J., Nyssen, J., and Van Beek, L.P.H. 2005. The effectiveness of hillshade maps and expert knowledge in mapping old deep-seated landslides. *Geomorphology*, Vol. 67, pp. 351–363.

Van Gaalen, K.E., Flanagan, L.B., and Peddle, D.R. 2007. Photosynthesis, chlorophyll fluorescence and spectral reflectance in Sphagnum moss at varying water contents. *Oecologia*, Vol. 153, pp. 19–28.

Verrelst, J., Schaepman, M.E., Koetz, B., and Kneubühler, M. 2008. Angular sensitivity analysis of vegetation indices derived from CHRIS/PROBA data. *Remote Sensing of Environment*, Vol. 112, pp. 2341–2353.

Walters, R.G. 2005. Towards an understanding of photosynthetic acclimation. *Journal of Experimental Botany*, Vol. 25, pp. 435–447.

Whitehead, D., and Gower, S.T. 2001. Photosynthesis and light-use efficiency by plants in a Canadian boreal forest ecosystem. *Tree Physiology*, Vol. 21, pp. 925–929.

Yuan, W., Liu, S., Zhou, G., Tieszen, L., Baldocchi, D., Bernhofer, C., Gholz, H., Hollinger, D.Y., Hu, Y., Law, B.E., Stoy, P.C., and Vesala, T. 2007. Deriving a light use efficiency model from eddy covariance flux data for predicting daily gross primary production across biomes. *Agricultural and Forest Meteorology*, Vol. 143, pp. 189–207.

Zarco-Tejada, P.J., Miller, J.R., Mohammed, G.H., Noland, T.L., and Sampson, P.H. 2002. Vegetation stress detection through chlorophyll a + b estimation and fluorescence effects on hyperspectral imagery. *Journal of Environmental Quality*, Vol. 31, pp. 1433–1441.

Zhang, H., Sharifi, M.R., and Nobel, P.S. 1995. Photosynthetic characteristics of sun versus shade plants of *Encelia farinosa* as affected by photosynthetic photon flux density, intercellular CO_2 concentration, leaf water potential, and leaf temperature. *Australian Journal of Plant Physiology*, Vol. 22, pp. 833–841.

Zhang, Q., Middleton, E.M., Margolis, H.A., Drolet, G.G., Barr, A.A., and Black, T.A. 2009. Can a satellite-derived estimate of the fraction of PAR absorbed by chlorophyll ($FAPAR_{chl}$) improve predictions of light-use efficiency and ecosystem photosynthesis for a boreal aspen forest? *Remote Sensing of Environment*, Vol. 113, No. 4, pp. 880–888.

